Fyn interrupts telomere maintenance in stem cells by phosphorylating menin at tyrosine 603

SOUREN PAUL (paulx215@umn.edu)
The Hormel Institute, University of Minnesota

Preston McCourt
The Hormel Institute, University of Minnesota

Le Thi My Le
The Hormel Institute, University of Minnesota https://orcid.org/0000-0002-0700-6064

Joohyun Ryu
The Hormel Institute, University of Minnesota

Wioletta Czaja
The Hormel Institute, University of Minnesota

Ann Bode
The Hormel Institute, University of Minnesota

Rafael Contreras-Galindo
University of Minnesota https://orcid.org/0000-0002-6284-3359

zigang Dong
Zhengzhou University https://orcid.org/0000-0002-4174-4028

Article

Keywords: Telomere, Stem cells, Telomerase, Dyskeratosis Congenita, Fyn

Posted Date: April 1st, 2022

DOI: https://doi.org/10.21203/rs.3.rs-1425640/v1

Abstract

Telomeres protect chromosome ends and determine the proliferative potential of cells. The canonical telomere sequence TTAGGG is synthesized by telomerase holoenzyme, which maintains telomere length in proliferative stem cells. Although the core components of telomerase are well defined, many aspects of telomerase regulation are poorly understood. We report a novel role for the Src family kinase Fyn, which interrupts telomere maintenance in stem cells by negatively regulating telomerase assembly. We determine that Fyn promotes SUMOylation of the scaffold protein menin at lysine 609 (K609) by phosphorylating menin at tyrosine 603 (Y603). We show that K609-SUMOylated menin associates with much greater affinity to the telomerase RNA component (TERC) and interferes with telomerase assembly by preventing dyskerin (DKC1) and H/ACA ribonucleoprotein complex subunit 1 (GAR1) from binding to TERC. Importantly, we find that inhibition of Fyn reduces telomere shortening in human iPSCs and mice harboring mutations for dyskeratosis congenita.

Introduction

Telomeres, regions of TTAGGG repeats at the ends of the chromosomes, shrink in somatic cells during cell replication[1]. Telomere shortening can be counteracted by telomerase holoenzyme, a ribonucleoprotein that maintains telomere length by synthesizing telomeric DNA[2]. Although telomerase activity is greatly reduced in somatic cells, it is upregulated in stem cells that undergo rapid expansion[3]. In telomere biology disorders (TBDs), such as dyskeratosis congenita (DC), telomerase or telomere maintenance is defective, which often causes bone marrow failure due to accelerated telomere shortening in hematopoietic stem cells[4]. Currently, there is no specific treatment for TBDs and transplantation comes with great risk and poses a number of challenges[5] .

Endogenous telomere maintenance is modulated by many mechanisms, including transcriptional regulation of telomerase reverse transcriptase (TERT) and TERC, post-translational regulation of TERT, and telomerase recruitment[6]. However, little is known about the role that kinases play in telomere maintenance, although previous evidences showed that ATM and ATR are positive regulators of telomere length[7,8]

Fyn is a Src family tyrosine kinase that phosphorylates multiple substrates and regulates many critical biological processes, including cell growth and survival[9,10]. Previous studies showed that Src family kinase inhibition prevents stem cell differentiation[11,12]. Here, we describe a critical role for Fyn, which negatively regulates telomere length in stem cells. We determined that genetic or pharmacological suppression of Fyn in mouse and human stem cells stabilizes telomere length. We also found that post-translational modifications of menin, a novel Fyn phosphorylation substrate, play crucial roles in Fyn-mediated telomere erosion. Named for its role in multiple endocrine neoplasia type 1 (MEN1) syndrome, menin is involved in many cellular processes, including transcriptional regulation, and can act as a cancer suppressor or promoter depending on the context[13]. A previous study showed that menin localizes to

telomeres in meiotic cells, but it does not directly interfere with telomerase activity in carcinoid cells[14]. We show that menin is phosphorylated by Fyn and undergoes phosphorylation-dependent SUMOylation, which increases binding to TERC and prohibits recruitment of telomerase subunits DKC1 and GAR1. Without proper recruitment of DKC1 and GAR1 to TERC, telomerase assembly and telomere elongation are reduced.

We demonstrate that pharmacological inhibition of Fyn or suppression of *Fyn* gene prevents accelerated telomere erosion in a DC mouse model with mutated TIN2, a shelterin complex subunit. We also demonstrate that Fyn knockout prevents accelerated telomere erosion in DC patient iPSCs that harbor a mutation in DKC1. Our findings indicate that Fyn inhibitors may be a viable therapeutic intervention for patients with TBDs.

Results

Fyn inhibition promotes telomere maintenance in mice and stem cells

We previously found that $Fyn^{-/-}$ mice produced larger and greater number of tumors after induction of skin carcinogenesis[9]. Other studies have focused on the role of Fyn in stem cell differentiation, finding that Src family kinase inhibition prevented stem cell differentiation[11,12]. Given that telomere maintenance is a critical component of both cancer and stem cell proliferation, we were curious to see how the absence of Fyn affected telomere length in $Fyn^{-/-}$ mouse tissue and stem cells. In a pilot study, we found that 43-week-old $Fyn^{-/-}$ female mice (n = 4) exhibited greater telomere length in liver, colon and skin tissues compared to wild type (WT) mice (Extended Fig. 1A, B, C). As previous reports showed that skin and gastrointestinal tract tissues are excellent sources of stem cells[15,16], we hypothesized that Fyn may negatively regulate telomere length in stem cells.

We tested this hypothesis in mESCs obtained from blastocysts of 43 weeks old WT and $Fyn^{-/-}$ mice or using Fyn shRNA interference in E14TG2a (E14) mESCs. (Fig. 1A-F, Extended Fig. 1D, E). Fyn knockout was confirmed by western blot (Fig. 1B). Cytogenetic analysis showed that telomeres in $Fyn^{-/-}$ stem cells are indeed longer than telomeres in WT stem cell metaphase spreads (Fig. 1A) or interphase nuclei (Fig. 1E) at passage 12. We performed Fyn knockdown in E14 mESCs using sh-RNA and confirmed knockdown by western blot (Fig. 1D). Sh-Fyn cells showed increased telomere length compared to sh-mock cells (Fig. 1C, F) at passage 18.

We used qRT-PCR and Flow-FISH to further confirm elongated telomeres in $Fyn^{-/-}$ mESCs cells and Fyn knockdown E14 cells (Extended Fig. 2A-F). The mean telomere fluorescence value was higher in Fyn-deficient ES cells than WT ES cells or mock-infected cells as determined by Flow-FISH (Extended Fig. 2A and C). A significantly higher telomere to single copy gene ratio (T/S) was observed in $Fyn^{-/-}$ ES cells (Extended Fig. 2B) and Fyn knockdown E14 cells (Extended Fig. 2D) compared to WT ES cells and sh-

mock cells, respectively. Notably, stable overexpression of *Fyn* in sh-Fyn E14 cells (Extended Fig. 2E) significantly reduced telomere FISH signals as compared to sh-Fyn cells (Extended Fig. 2F), suggesting that the level of active Fyn imposes a negative impact on telomeres.

We further asked whether $Fyn^{-/-}$ mice maintained telomeres at old age. Genotyping and IHC analysis confirmed Fyn knockout in colon and skin tissues of 97-week-old $Fyn^{-/-}$ mice (Extended Fig. 3A, B, C). Q-FISH analysis showed that telomere length in $Fyn^{-/-}$ mice was elongated in both male and female mice compared to WT mice (Fig. 1G). Taken together with the *in vitro* stem cell data and earlier 43-week-old $Fyn^{-/-}$ mice data, these results indicate that Fyn is a negative regulator of mammalian telomere length in stem cells, regardless of age and gender.

Fyn does not inhibit telomerase activity in vitro

To elucidate the molecular mechanism of Fyn-mediated telomere erosion, we performed Fyn and telomerase reverse transcriptase (TERT) immunoprecipitation in WT mESCs lysates. To our surprise, TERT was detected in the anti-Fyn-precipitated complex (Extended Fig. 4A). We also detected endogenous Fyn in TERT pulldown complex (Extended Fig. 4B). To evaluate whether Fyn phosphorylates TERT, we conducted an *in vitro* kinase assay using a recombinant human TERT purified from *E. Coli* expression system (aa 787–1084), [γ^{32}P]ATP, and active Fyn. β-catenin was used as a positive control for Fyn phosphorylation. However, autoradiography determined that Fyn does not phosphorylate TERT (Extended Fig. 4C).

We measured telomerase reverse transcriptase (TERT) expression and found no difference between $Fyn^{-/-}$ and WT stem cells or between Fyn knockdown and sh-mock stem cells (Fig. 2A, B). Therefore, the elongated telomeres found in $Fyn^{-/-}$ and Fyn knockdown stem cells appears not be the result of a change in TERT expression. To evaluate whether Fyn directly interferes with telomerase activity, we measured telomerase activity by the telomere repeat amplification protocol (TRAP), an assay that provides a telomere-imitating oligonucleotide substrate for endogenous telomerase to perform telomere DNA synthesis *in vitro*[17]. The TRAP assay is helpful for measuring telomerase activity, but does not incorporate endogenous TERC and cannot detect improper localization of telomerase subunits[18]. There was no significant difference in telomerase activity between Fyn KO and WT mESCs (Fig. 2C), sh-Fyn and sh-mock E14 cells (Fig. 2D), or colon lysates of $Fyn^{+/+}$ and $Fyn^{-/-}$ mice (Fig. 2E). Thus, Fyn might not directly interfere with TERT expression or telomerase activity. Rather, this data suggests that Fyn interferes with endogenous telomere maintenance indirectly.

Fyn phosphorylates menin at tyrosine 603

After discovering that Fyn does not directly interfere with TERT expression or telomerase activity, we screened a candidate list of transcription factors or their isoforms known to be related to telomere maintenance (Extended Table 1)[19]. We performed Fyn immunoprecipitation with WT mESCs lysates using an anti-Fyn antibody and blotted against the candidate proteins. Of the candidate proteins, only the scaffold protein menin showed significant interaction with Fyn (Extended Fig. 4D). Endogenous menin

was detected in anti-Fyn-precipitated protein complexes in both E14 cells (Fig. 3A) and WT mESCs isolated from mice (Fig. 3B). We performed the previously described *in vitro* kinase assay with full-length recombinant human menin purified from wheat germ expression system and found that Fyn does indeed phosphorylate menin (Fig. 3C). Tandem mass spectrometry analysis identified menin Y603 as the site of Fyn phosphorylation (Fig. 3D).

We performed an additional *in vitro* kinase assay with active Fyn to compare WT and mutant menin (menin Y603F). The assay showed that phosphorylation of menin Y603F is greatly decreased (Fig. 3E), confirming that Y603 serves as a site of Fyn phosphorylation.

A previous study described menin as a cell-type specific negative regulator of TERT transcription, but overexpression of menin did not significantly reduce *in vitro* telomerase activity[20]. Although we found that Fyn deletion or inhibition did not affect TERT expression or *in vitro* telomerase activity (Fig. 2), we evaluated whether Fyn's phosphorylation of menin is involved with TERT transcription in stem cells. We performed a chromatin-immunoprecipitation assay using anti-menin antibody in sh-mock vs sh-Fyn E14 cells. qPCR of the TERT promoter showed no significant difference in menin occupancy between sh-mock vs sh-Fyn E14 nuclear lysates (Extended Fig. 4E). We concluded that Fyn-mediated phosphorylation of menin does not appear to regulate TERT transcription in stem cells.

Phosphorylation of menin at Y603 promotes its SUMOylation and stability

We further studied whether Fyn regulates menin stability. We studied whether menin is affected by SUMOylation, which is known to affect stability, localization, and transcriptional regulation activity of menin[21]. A phosphorylation-dependent SUMOylation consensus motif has previously been reported[22]. Another report showed SUMO-modification of menin at K591 and suggested that menin contains multiple SUMOylation sites[23]. We proceeded to investigate whether phosphorylation of menin at Y603 regulates its SUMOylation.

We performed immunoprecipitation with anti-menin antibody and blotted against SUMO-1 and SUMO-2/3/4. Results showed that menin interacted with SUMO-1 in sh-mock cells, but the interaction was greatly reduced in sh-Fyn cells (Fig. 4A), suggesting that Fyn-mediated phosphorylation regulates menin's interaction with SUMO-1. No interaction of menin with SUMO-2/3/4 was observed (Fig. 4B). SUMOylation intensity was assessed in nuclear lysates from mESCs. We observed a reduced SUMOylation intensity in Fyn-knockout cells vs. WT cells. Moreover, SUMOylation intensity was also reduced in sh-Fyn mESCs (Fig. 4C).

To gain insight into the mechanism of Fyn-mediated menin SUMOylation, we transfected HEK 293T cells with Xpress-tagged pcDNA-Wt-*MEN1 (*Wt-*MEN1),* pcDNA-Y603F-*MEN1* (Y603F-*MEN1*), and pcDNA-Y603D-*MEN1* (Y603D-*MEN1)* with or without pcDNA-HA-*SUMO-1(SUMO-1)*. Menin Y603D served as a phosphomimetic mutant. No SUMOylation bands were observed in cells transfected with Wt-*MEN1* only or in cells co-transfected with mock vector and *SUMO-1* (Fig. 4D). In SUMO-1 co-transfection experiments, SUMOylation was observed in both Wt-*MEN1* and Y603D-*MEN1*-transfected cells, but

SUMOylation was reduced significantly in Y603F-*MEN1*-transfected cells (Fig. 4D). The reduced SUMOylation signal in Y603F-*MEN1*-transfected cells shows that menin SUMOylation is phosphorylation-dependent (Fig. 4D).

We also compared expression of WT, Y603F, and Y603D menin with or without *SUMO-1* in cytoplasmic and nuclear extracts. The ratio of cytoplasmic to nuclear menin expression did not change between WT and mutant menin. However, Y603F-*MEN1*-transfected cells showed decreased menin expression in cytoplasm and nucleus compared to WT-*MEN1* (Fig. 4E). And, interestingly, Y603D-*MEN1* plus *SUMO-1* co-transfected cells showed increased menin expression in cytoplasm and nucleus compared to WT-*MEN1* plus SUMO-1 co-transfected cells (Fig. 4E). These results show that phosphorylation-dependent SUMOylation of menin promotes its stability, but nuclear localization does not appear to be dependent on phosphorylation or SUMOylation.

Menin is SUMOylated at lysine 609

To further study phosphorylation-dependent SUMOylation of menin, we used GPS-SUMO (http://sumosp.biocuckoo.org/) to identify probable SUMOylation site(s)[24]. We selected lysines with the lowest p-value, 493 (K493) and 609 (K609) (Fig. 5A) and performed co-transfections with SUMO-1 and SUMOylation-deficient menin mutants K493R or K609R. SUMOylation efficacy was reduced in K493R-*MEN1*-transfected cells and completely abolished in K609R-*MEN1*-transfected cells (Fig. 5B). This result confirmed the existence of multiple SUMOylation sites on menin, although K493 SUMOylation appears to be a passive SUMO site similar to K591[23]. We used a SUMOylation assay kit to detect SUMOylation in cells co-transfected with *SUMO-1* and WT, Y603F, Y603D, or K609R menin. Co-transfection of Y603D-*MEN1* and *SUMO-1* indeed increased Menin's SUMOylation (Fig. 5C). SUMOylation intensity was decreased in Y603F-*MEN1* plus *SUMO*-1 co-transfected cells compared to Y603D-*MEN1* plus *SUMO-1* co-transfected cells. Consistent with the previous result, SUMOylation intensity was reduced significantly in K609R-*MEN1* plus *SUMO-1* co-transfected cells compared to Wt, Y603F, and Y603D mutant plus *SUMO-1* transfected cells (Fig. 5C).

Telomere length is greater in stem cells that express Y603F menin or K609R menin

Based on the above results, we hypothesized that phosphorylation-dependent SUMOylation of menin may have an inhibitory effect on telomere maintenance. To test this observation, WT or mutant plasmids of *MEN1* were electroporated with *SUMO-1* into Fyn knockdown E14 cells. Stable Fyn knockdown E14 cells (Fig. 5D) harboring a phospho-site mutant of menin (Y603F) or SUMO-site mutant of menin (K609R) showed significantly increased telomere length compared to mock, WT, or phospho-mimic (Y603D)-transfected cells (Fig. 5E). Consistent with the fluorescence data, T/S ratio in the phospho-deficient mutant and SUMO-mutant cells was also significantly higher compared to mock, WT, or phospho-mimic mutant cells. No significant difference in the length of the telomeres was noted between mock, WT, or Y603D-transfected cells (Fig. 5F).

SUMOylated menin is associated with TERC *in vitro*

We next tested whether menin binds to TERT directly. Immunoprecipitation results showed that menin is not a binding partner with TERT (Extended Fig. 5). We next investigated whether menin interacts with the telomeric RNA component (TERC) using an *in vitro* RNA pulldown assay with nuclear lysates from ES cells, transfected HEK 293T cells, and *in vitro* transcribed biotinylated TERC. First, we confirmed the biotinylation of TERC in HeLa cell lysates. The assay showed that DKC1, a protein that binds directly to TERC, was only pulled down with streptavidin agarose beads when the biotin moiety was present (Extended Fig 6A). Western blotting from two independent experiments revealed that menin was present in the TERC pulldown complex. Interestingly, menin showed greater association with TERC in WT ES cells vs $Fyn^{-/-}$ cells (Fig. 6A). RNA pulldown assays with co-overexpressed Wt and mutant *MEN1* with *SUMO-1* showed similar results. We detected significantly higher menin in TERC pulldown complexes of Y603D-*MEN1* plus *SUMO-1*-transfected cells. Although negligible binding was observed in other transfections, no binding was detected in the K609R plus SUMO-1 transfection. (Fig. 6B).

To confirm this observation, we performed an RNP pulldown assay with menin or Xpress antibodies and evaluated TERC expression by qRT-PCR (Fig. 6C, D). RNP pulldown with anti-menin antibodies (Fig. 6C) demonstrated that TERC expression was substantially higher in the WT ES RNP complex compared to the $Fyn^{-/-}$ ES RNP complex. Similarly, TERC association was higher in the RNP complex Y603D-*MEN1* and *SUMO-1* co-transfected cells compared to the RNP complex WT-*MEN1*- or Y603F-*MEN1* plus *SUMO-1*-transfected cells. K609R-*MEN1* and *SUMO-1* co-transfected cells showed much lower expression of TERC in the RNP complex (Fig. 6D).

We next performed Immunofluorecence-Fluorescent *in situ* hybridization (IF-FISH) with anti-menin antibody and a telomere FISH probe in metaphase spread chromosomes. Results confirm the co-localization of telomere and menin at some chromosomes (Extended Fig. 6B). Significantly higher co-localization of menin at telomeric DNA was observed in WT stem cells, whereas $Fyn^{-/-}$ ES cells showed negligible co-localization (Extended Fig. 6B, right). We detected menin at other chromosome locations as well, which affirms menin's role as an epigenetic regulator.

SUMOylated menin prevents recruitment of DKC1 and GAR1 to TERC

Tandem mass spectrometric analysis of the TERC pull-down complex from Y603F-*MEN1* plus *SUMO-1* co-transfected HEK 293T cell nuclear lysates, indicated that 54 human proteins were associated with TERC in Y603F-*MEN1*-transfected cells. The number of proteins was reduced dramatically in Y603D-*MEN1* and *SUMO-1* co-transfected cells (Fig. 7A, Extended Table 2). Importantly, Y603D-*MEN1* transfection prohibited the recruitment of TERC-associated protein members, GAR1 and DKC1 (Fig. 7B, Extended Table 2), which are required for telomere maintenance[25].

TERC-IP followed by Western blotting confirmed that DKC1 and GAR1 TERC binding was reduced in nuclear lysates of Y603D-*MEN1*+SUMO-1 transfected cells compared to nuclear lysates of Y603F-*MEN1*+SUMO-1 transfected cells (Fig. 7C). We also compared DKC1 and GAR1 expression in TERC-IP of nuclear lysates of 293T cells transfected with Y603D-*MEN1*+SUMO-1 or K609R-*MEN1*+SUMO-1. We

found that cells transfected with menin mutant (K609R), which is not SUMOylated (Fig. 6B), showed greater DKC1 and GAR1 binding in TERC-IP (Fig. 7D). Xpress-tagged menin binding was also reduced, further supporting that SUMOylation of menin at K609 promotes its association with TERC (Fig. 7D). These results show that association of SUMOylated menin with TERC restricts the recruitment of DKC1 and GAR1. Thus, when SUMOylated menin associates with TERC, it inhibits telomere maintenance by preventing localization of telomerase subunits. Moreover, in the absence of Fyn, unSUMOylated menin does not inhibit telomere maintenance.

Inhibition of Fyn prevents telomere erosion in $TIN2^{+/DC}$ mice

Dyskeratosis congenita (DC) is a TBD characterized by accelerated telomere shortening caused by mutations in telomerase subunits, trafficking components, or the shelterin complex[26]. $TIN2^{+/DC}$ mice are a DC animal model that exhibit accelerated telomere shortening due to a mono-allelic mutation in TIN2, a shelterin complex subunit[27]. We generated $TIN2^{+/DC}$, $Fyn^{+/+}$ and $TIN2^{+/DC}$, $Fyn^{+/-}$ mice to study the effect of Fyn inhibition on accelerated telomere shortening (Extended Fig. 7A and B). Interestingly, $TIN2^{+/DC}$, $Fyn^{-/-}$ mice were not viable (Extended Fig. 7B). We used immunofluorescence to measure Fyn expression in 6-month-old bone marrow and found that $TIN2^{+/DC}$-$Fyn^{+/-}$ mice had lower Fyn expression than $TIN2^{+/DC}$-$Fyn^{+/+}$ mice (Extended Fig. 7C and D). A previous study showed that Fyn phosphorylates β-catenin at Y142[28]. We measured pY142-β-catenin immunofluorescence to evaluate the catalytic activity of Fyn in $TIN2^{+/DC}$-$Fyn^{+/-}$ and $TIN2^{+/DC}$-$Fyn^{+/+}$ bone marrow. $TIN2^{+/DC}$-$Fyn^{+/-}$ mice showed lower pY142-β-catenin expression (Extended Fig. 7C and E). Therefore, monoallelic deletion of Fyn was sufficient to reduce both Fyn expression and catalytic activity. However, we were not able to identify pancytopenia in bone marrow H&E staining of $TIN2^{+/DC}$-$Fyn^{+/-}$ or $TIN2^{+/DC}$-$Fyn^{+/+}$ mice (Extended Fig. 7F). We proceeded to evaluate telomere length in 6-month-old $TIN2^{+/DC}$, $Fyn^{+/+}$ vs. $TIN2^{+/DC}$, $Fyn^{+/-}$ female mice. Flow-FISH results showed that telomeres were significantly elongated in bone-marrow cells of $TIN2^{+/DC}$-$Fyn^{+/-}$ mice vs. $TIN2^{+/DC}$-$Fyn^{+/+}$ mice (Fig. 8A). $TIN2^{+/+}$-$Fyn^{+/+}$ mice showed a small, but not significant decrease in telomere length compared to control $TIN2^{+/+}$-$Fyn^{+/-}$ mice (Fig. 8A). Q-FISH analysis of bone marrow biopsy samples revealed a higher number of telomere foci in $TIN2^{+/DC}$-$Fyn^{+/-}$ mice vs. $TIN2^{+/DC}$-$Fyn^{+/+}$ mice (Fig. 8B). We also measured pY603-menin expression in bone marrow, using a custom antibody (E1171) purified from a rabbit in-house at Abclonal (Supplementary text). The purified antibody was validated for specificity (Extended Fig. 8A-D) before use in any experiment. pY603-menin protein expression was reduced in bone marrow of $TIN2^{+/DC}$-$Fyn^{+/-}$ mice vs. $TIN2^{+/DC}$-$Fyn^{+/+}$ mice (Fig. 8C).

To further confirm a possible role of Fyn in telomere shortening, we pharmacologically inhibited Fyn by treating $TIN2^{+/DC}$ mice with vehicle or 3 mg/kg of Src-family kinase inhibitor PP2 intraperitoneally every day for two months. PP2 was chosen because it inhibits Fyn with higher specificity than other Src family kinases, and therefore has less off-target effects[29]. Flow-FISH and Q-FISH data revealed that the telomeres of vehicle-treated $TIN2^{+/DC}$ mice went through a significant shortening in contrast to the telomeres of mice treated with PP2 (Fig. 8D, E, F). $TIN2^{+/+}$ control female mice did not show any

significant difference in telomere length between sham and PP2 treatment (Fig. 8D). Reduction of Fyn activity was confirmed by measuring pY142-β-catenin expression (Extended Fig. 9A, B, C). Consistent with our previous animal experiment, no sign of bone marrow failure was observed (Extended Fig. 9D). Immunohistochemistry showed that PP2 treatment reduced pY603-menin protein expression in bone marrow samples isolated from both male and female mice (Fig. 8G).

Fyn inhibition attenuates telomere shortening in TIN2$^{+/DC}$ MEFs

Accelerated telomere shortening was also reversed with Fyn inhibition, in mouse embryonic fibroblasts (MEFs) derived from littermate embryos of the TIN2$^{+/DC}$ genotype (Fig. 9A). MEFs isolated from embryos 1 and 4 were positive for TIN2 mutation and the *Cre* transgene. MEFs from embryo 1 were used for further experiments. Early passage MEFs were used to knock down the *Fyn* gene, which was confirmed by western blot (Fig. 9B). Expression of pY603-menin was also reduced in sh-Fyn MEFs vs. sh-mock MEFs (Fig. 9B) Remarkably, TIN2$^{+/DC}$-sh-Fyn MEFs showed a significantly higher telomere signal after only 6 passages (Fig. 9C).

Fyn knockout in Human DC iPSCs attenuates telomere shortening

We next investigated Fyn inhibition in iPSCs from a DC patient that exhibit accelerated telomere erosion and telomerase deficiency due to a mutation in DKC1. We first used DC fibroblasts to generate DC iPSCs. iPSC generation was confirmed by the expression of SSEA-4, Tra-1-60, Oct4 and Nanong (Extended Fig. 10A and B). Next, we attempted to create DC iPSCs with Fyn KO using CRISPR-Cas9. A mock CRISPR-Cas9 plasmid was used as negative control. CRISPR-Cas9 transduction generated a population of iPSCs with significantly decreased Fyn expression, although expression was not completely abolished in the whole population of cells (Fig. 10A). CRISPR-Cas9-mediated Fyn knockdown (KD) reduced both Fyn and pY603-menin expression in DC iPSCs (Fig. 10A, B). iPSCs showed no significant difference in telomere length after 3 passages (Fig. 10C). However, at passage 12, Fyn KD iPSCs showed significantly longer telomeres than mock iPSCs as determined by Q-FISH (Fig. 10D). Consistent with these results, Flow-FISH and qRT-PCR results showed that Fyn$^{-/-}$ DC iPSCs exhibited significantly higher telomere signals compared to control DC iPSC after 12 passages (Fig. 10E and F, respectively).

Discussion

This work uncovers a new mechanism of telomere maintenance in mammalian stem cells. We demonstrate that Fyn, an Src-family kinase, is a negative regulator of mammalian telomere length. We first discovered that inhibition or deletion of Fyn stabilizes telomere length. However, we found that Fyn does not affect TERT expression and does not interfere with telomerase activity. Rather, Fyn negatively regulates endogenous telomere length by phosphorylating menin at Y603.

Phosphorylation of menin at Y603 promotes phosphorylation-dependent SUMOylation at K609, which increases menin's stability and association with TERC. Importantly, phospho-site mutant Y603F and SUMO-site mutant K609R menin showed decreased SUMOylation and stability, but increased telomere

signal *in vitro*. We found that SUMO-modified menin associates much more strongly with TERC, and this association prevents telomerase subunits DKC1 and GAR1 from binding to TERC. As DKC1 and GAR1 are essential components of telomerase holoenzyme[30], we propose that SUMOylated menin competitively binds to TERC and ultimately prevents telomere elongation by reducing telomerase holoenzyme assembly and/or stability. The inhibitory role of menin-TERC binding on telomere lengthening, despite the presence of TERT, affirms the importance of TERC and telomerase assembly during telomere elongation in TERT-expressing cells[31].

In humans, defective telomerase or telomere maintenance may result in a TBD such as DC [5,32,33]. Our data from TIN2$^{+/DC}$ Fyn$^{+/-}$ isolated bone marrow shows that mono-allelic deletion of Fyn is sufficient to reduce its expression and kinase activity. Importantly, mono-allelic deletion was also sufficient to reduce pY603-menin expression and telomere shortening. The pharmacological inhibitor of Fyn, PP2, produced similar results in TIN2$^{+/DC}$ mice. But most striking was the reduction of telomere shortening in sh-Fyn transduced TIN2$^{+/DC}$ MEFs after only 6 passages. Although MEFs have telomerase activity[34], it would be most interesting to study the effects of Fyn inhibition in TIN2$^{+/DC}$ mTR$^{-/-}$ MEFs that exhibit telomerase-independent accelerated telomere shortening[27].

We also show that CRISPR-Cas9-mediated Fyn inhibition in mutant DKC1 human DC iPSC stabilized telomeres concurrent with a decline in pY603-menin expression. It is tempting to speculate that SUMOylated menin exacerbates telomere shortening by further inhibiting telomerase assembly in these telomerase-defective human iPSCs. Moreover, our human iPSC data suggests that Fyn negatively regulates telomere maintenance even in the presence of defective telomerase.

In conclusion, our results demonstrate that Fyn-mediated phosphorylation and subsequent SUMOylation of menin disrupts telomere maintenance in proliferating stem cells. Inhibition or deletion of Fyn promotes telomere maintenance, even in telomerase-defective stem cells. Fyn inhibitors may be a viable treatment options for DC or other TBDs, although the development of specific inhibitors is needed.

Materials And Methods

The antibodies, primers, kits, and chemicals used in this study are in extended tables 3–6.

Fyn $^{-/-}$ animal model

Fyn$^{-/-}$ mice (B6.129S7-Fyntm1Sor/J) were purchased from The Jackson laboratory[35] and bred, propagated, and maintained at The Hormel Institute, University of Minnesota. Mice were maintained under conditions based on the guidelines established by the University of Minnesota Institutional Animal Care and Use Committee. Genotyping was performed using a standard protocol and Agilent Taq polymerase. Representative genotyping is presented in Extended Fig. 2A. Age matched (± 4 days) wildtype and Fyn$^{-/-}$ mice (n = 12 males + 12 females) were maintained for 97 weeks. Some mice were euthanized based on veterinary advice and the study ended with 13 mice (6 males + 7 females).

Generation of mouse embryonic stem cells (mESCs) from WT and Fyn$^{-/-}$ mice

mESCs were generated from the inner cell mass of blastocysts isolated from 3.5 days post coitum mice[36]. Briefly, a feeder layer of mouse embryonic fibroblasts (MEFs, 1x10^6) was plated two days before blastocyst isolation. MEFs were then treated with mitomycin C (10 µg/ml) for 2 h. Isolated blastocysts were washed once with KnockOut™ Dulbecco's Modified Eagle Medium (DMEM) and transferred aseptically on a feeder layer with KnockOut™ DMEM supplemented with 20% knockout serum replacement and 1000 U/mL Leukemia Inhibitory Factor (LIF). After 48 h the medium was changed and blastocysts were left to hatch for 7–10 days. Cells from hatched blastocysts were transferred to a new feeder layer. Colonies generated from the previous step were transferred onto a new feeder layer. Stem cells were confirmed by alkaline phosphatase (AP) staining and Western blotting for Sox2 and KLF4 (Extended Fig. 1D and E).

Cell culture

mESCs (E14Tg2a) were maintained in DMEM supplemented with 15% heat-inactivated ESC-qualified fetal bovine serum (FBS), 0.055 mM β-mercaptoethanol, 2 mM L-glutamine, 0.1 mM minimum essential medium non-essential amino acids, and 1,000 U/mL LIF.

Generation of TIN2-DC conditional mice and PP2 treatment

TIN2-DC conditional mice (B6(Cg)-Tinf2tm2.1Tdl/J) and Cre-recombinase expression [Tg(CMV-cre)1Cgn] were purchased from The Jackson laboratory. TIN2$^{+/DC}$ mice were generated by crossing TIN2$^{+/DC\text{-}COND}$ mice with Cre-recombinase expressing mice. TIN2$^{+/DC\text{-}COND}$ mice were also bred with Fyn$^{-/-}$ mice and subsequently crossed with Cre-recombinase expressing mice to obtain TIN2$^{+/DC}$- Fyn$^{-/-}$ double knockout mice. TIN2$^{+/DC}$- Fyn$^{-/-}$ mice were not obtained possibly due to embryonic lethality of Fyn double knockout in TIN2$^{+/DC}$ mice. Nonetheless, TIN2$^{+/DC}$- Fyn$^{+/-}$ mice were generated (Extended Fig. 7B). The third generation TIN2$^{+/DC}$ mice were used for experiments. Representative images of genotyping of these mice are shown (Extended Fig. 7A).

TIN2-Fyn double knockout age matched-female mice (± 4 days) were divided into 4 groups: experimental groups TIN2$^{+/DC}$- Fyn$^{-/+}$ (n = 8) and TIN2$^{+/DC}$-Fyn$^{+/+}$ (n = 8) and negative controls TIN2$^{+/+}$-Fyn$^{+/+}$ (n = 4) and TIN2$^{+/+}$- Fyn$^{+/-}$ (n = 4). A sufficient number of male mice appropriate for statistical analysis was not generated, and thus, only females were included in the study. These mice were maintained for 24 weeks before euthanization.

PP2 (3-(4-chlorophenyl)-1-(1,1-dimethylethyl)-1H-pyrazolo[3,4-d]pyrimidin-4-amine) is a potent SFK inhibitor that blocks Fyn activity (IC_{50} = 5 nM)[37]. We used PP2 as a Fyn inhibitor in mice at a dose of 3 mg/kg. This dose of PP2 was safe for mice and did not lead to toxicity or death. Age-matched TIN2$^{+/DC}$ mice (± 4 days) were divided into 2 groups (n = 12, 6 males + 6 females) and treated with vehicle or PP2

for 60 days *i.p.* TIN2$^{+/+}$mice (n = 6, females) were also divided into 2 groups and treated similarly with vehicle or PP2 and served as controls.

Mouse embryonic fibroblast (MEF) collection from TIN2$^{+/DC}$ mouse embryos

MEFs were collected from freshly harvested 13.5 dpc TIN2$^{+/DC}$ embryos following a published protocol[38]. Briefly, harvested embryos were washed with PBS and placental and maternal tissues removed. Embryo heads were saved for genotyping. Embryos were placed in a separate 10 cm^2 dish and minced with 1 mL trypsin with sterile surgical blade. Isolated cells were incubated at 37°C for 45 min, and then maintained in MEF media (DMEM with 10% FBS). Suspended cells were transferred into a new flask with complete media and MEFs were grown to 80% confluence. Only MEFs having mutations in TIN2 and *Cre* transgene were used for further experiments.

Generation of DC-iPSCs from fibroblasts

DC fibroblasts were purchased from The Coriell Cell Repositories and maintained in MEM medium supplemented with 15% FBS and 1% non-essential amino acids. Induced pluripotent stem cells (iPSCs) were generated from DC fibroblasts by ectopic expression of Yamanaka transcription factors, Oct4, Klf4, Sox2, and c-Myc (OKSM), with the help of a STEMCCA Constitutive Polycistronic (OKSM) Lentivirus according to the manufacturer's protocol (MilliporeSigma). Briefly, 1 x10^6 DC fibroblasts were seeded onto gelatin-coated plates and infected with STEMCCA virus. Infected cells were then transferred to a plate containing 1 x 10^5 feeder cells. iPSC colonies were picked 25–30 days' post-infection and maintained in feeder-free E8 media (StemCell Technologies) on a Matrigel (Corning). Pluripotency was confirmed by Immunofluorescence and Western blotting with human iPSC specific markers.

Alkaline phosphatase (AP) staining

To perform AP staining, mESCs were cultured in the appropriate medium, fixed with 4% paraformaldehyde in phosphate buffered saline (PBS) for 2 min at room temperature. AP staining was performed using the Alkaline Phosphatase Detection Kit following the manufacturer's protocol (MilliporeSigma).

RNA interference of Fyn

To generate knockdown Fyn cells, pLKO.1-sh-Fyn, or pLKO.1-mock lentivirus plasmids were co-transfected with psPAX2 and pMD2.0G into HEK 293T cells by using the iMFectin transfection reagents (GenDepot). The mouse lentiviral vector sequences for Fyn were purchased from the University of Minnesota Genomic Center. Viral particles containing 4 μg/mL polybrene were infected twice into E14TG2a cells at 24 h and 48 h of culture. After 48 h E14TG2a cells were selected with 1 μg/mL puromycin. Selected cells were maintained in complete media until reaching 80% confluence.

Telomeric repeat amplification protocol (TRAP) assay

TRAP assay was used to determine telomerase activity according to the manufacturer's recommendation (MilliporeSigma). Briefly, whole-cell lysates were prepared from wildtype, $Fyn^{-/-}$ mESCs, mock-, and sh-Fyn-transfected E14TG2a cells, and colon tissues of wildtype and $Fyn^{-/-}$ mice by using CHAPS lysis buffer. CHAPS-containing cell lysates (500 ng/μL) were used for the TRAP assay. Relative telomerase activity was determined from a TSR8 standard curve according to the manufacturer's protocol.

Quantitative *fluorescent in situ hybridization (Q-FISH) and flow cytometry-FISH (Flow-FISH) assays*

Q-FISH of metaphase chromosomes, interphase nuclei, and mouse tissue was performed as previously described[39]. Briefly, 1 μg/mL Colcemid (Cayman Chemicals) -treated and untreated cells were permeabilized with 75 mM KCl hypotonic solution followed by fixation using Carnoy's fixative. For tissue samples, deparaffinization of 5 μM sections of paraffin-embedded mouse organ specimens were conducted using standard protocols. Telomere Q-FISH staining was performed using TelC-Alexa-488 or TelG-Cy3 PNA telomere probes (PNA Bio Inc). Slides were counterstained with DAPI (Electron Microscopy Sci.) and visualized using Nikon or Zeiss LSM 900 confocal microscopes. Telomeres were analysed by using open-source software (Telometer; http://demarzolab.pathology.jhmi.edu/telometer/), as previously described[40].

Flow-FISH analysis was performed [41] with slight modifications. Briefly, cells (0.5×10^6) were washed in PBS containing 0.1% BSA and suspended in 300 μL hybridization buffer (70% formamide, 20 mM Tris-HCl, pH 7.0, 1% blocking reagent, 1 μg/mL PNA probe) and incubated for 2 h at RT. Cells were then washed twice with fixation buffer (60% formamide, 10 mM Tris-HCl, pH 7.0, 0.1% blocking reagent, 0.1% Tween 20) at 40°C, resuspended in PBS containing 0.1% BSA with 0.05 ug/mL of propidium iodide (PI) and analyzed by BD-FACS (BD Aria III). TelC-Alexa-488 PNA probe and PI nuclear stain was used in all flow-FISH analysis, except CRISPR-Cas9 transfected cells, where TelG-Cy3 PNA probe and DAPI were used instead.

q-PCR assay for telomere measurement in cells

Average telomere length was measured from genomic DNA of mouse or human stem cells by using a qPCR method previously described[42]. The single-copy genes *m36B4* and *h36B4* and the multicopy gene *hAlu* were used as references. 10 μL of 2×SYBR Green mix, 0.5 μL each of 10 μM forward and reverse primers, 4 μL DNase/RNase free water, and 5 μL genomic DNA (8 ng/μL) were mixed to obtain a 20 μL reaction. The qPCR was carried out in a Bio-Rad thermocycler (CFX96) with reaction conditions of 95°C for 10 min followed by 40 cycles of denaturation at 95°C for 15 s, 60°C annealing for 30 s, and 72°C extension and data collection for 30 sec. The CFX manager software was used to generate standard curves. The average telomere length is termed as the telomere to single copy gene (T/S) ratio.

Protein extraction, Western blotting, and Immunohistochemistry (IHC)

Cells were lysed withNP-40 lysis buffer (50 mM Tris-HCl, pH 7.6, 150 mM NaCl, 5 mM EDTA, 1% Nonidet P-40 with a protease inhibitor cocktail). Nuclear and Cytoplasmic fractions were obtained using the NE-

PER cytoplasmic and nuclear protein extraction kit (ThermoFisher Scientific). A phosphatase inhibitor cocktail was used for phosphoprotein analysis, and N-ethylmaleimide (NEM) was used for SUMO-protein analysis. The proteins were resolved in SDS-PAGE and transferred to polyvinylidene difluoride (PVDF) membranes. The membranes were blocked with 5% milk, and target proteins were detected with specific antibodies and visualized by chemiluminescence.

IHC was performed using a standard protocol. Paraffin-embedded tissues were subjected to deparaffination and antibody retrieval. Tissue sections were blocked with 10% goat-serum followed by overnight incubation with a primary antibody at 4°C. Slides were incubated with a secondary antibody and stained with 3,3'-Diaminobenzidine (DAB). For IF, a fluorochrome-conjugated secondary antibody was used instead. Images were quantified using ImageJ2 software[43].

Immunoprecipitation

A total amount of 1 mg of cell lysates in a volume of 500 µL were immunoprecipitated with 2 µg of each respective antibody and samples were rotated overnight at 4°C. 40 µL of protein A/G Sepharose beads (GenDepot) were added to each sample and rotated for 1 h at 4°C. Beads were washed 3 times with lysis buffer, and the supernatant fraction was analyzed by Western blotting.

Chromatin immunoprecipitation assay

Stable sh-mock and sh-Fyn E14 cells were seeded in 10 cm^2 plates. Chromatin immunoprecipitation (ChIP) was performed using the One-Day Chromatin Immunoprecipitation Kit (Magna ChIP G, MilliporeSigma) according to the manufacturer's protocol. Chromatin samples were immunoprecipitated with anti-menin antibody overnight at 4℃. The DNA fractions for TERT promoter was analyzed by qPCR.

Protein expression, purification and in vitro kinase assay

WT and mutant *MEN1* (Y603F) were cloned into pGEX-5X1 vector upstream a C-terminal 6×His tag. Menin WT and mutant (Y603F) proteins were expressed in *E. coli* BL21(DE3) pLysS cells (Promega). Cells were grown in Lysogeny broth to an OD 600 of 0.5-0.7 and protein expression was induced with 0.5 mM IPTG for 20 h at 16°C. Cells (200 mL) were pelleted at 7,000 rpm and resuspended in 10 mL lysis buffer (50 mM HEPES pH 8.0, 500 mM NaCl, 20 mM imidazole, 10% glycerol, 2 mM TCEP, 1% Tween-20, 1X protease inhibitor). Cell suspensions were incubated with lysozyme for 30 min and disrupted by sonication for 10 min. Cells were centrifuged for 30 min at 13,000 rpm, and lysates were equilibrated with Ni-NTA agarose beads (ThermoFisher Scientific) for 2 h at 4°C. Samples were centrifuged at 1,000 rpm for 3 min to remove the supernatant fraction. Beads were washed with 10 mL buffer 1 (50 mM HEPES pH 8.0, 500 mM NaCl, 30 mM imidazole, 10% glycerol, 0.5% Tween-20, 2 mM DTT), and 2X with 10 mL buffer 2 (50 mM HEPES pH 8.0, 500 mM NaCl, 40 mM imidazole, 10% glycerol, 0.5% Tween-20, 2 mM DTT). Proteins were eluted 3X with 0.1 mL elution buffer (50 mM HEPES pH 8.0, 150 mM NaCl, 300 mM imidazole) and transferred to kinase buffer (50 mM Tris pH 8.0, 100 mM NaCl) using Zeba Spin Desalting

columns (ThermoFisher Scientific). Proteins were separated by SDS-PAGE and stained with Coomassie blue. The protein concentrations were quantified using a Nanodrop at A280 (ThermoFisher Scientific).

Fyn protein with or without Menin recombinant protein (WT and mutant) was incubated for 30 min in a 30°C water bath. Proteins were incubated with 10 µCi [γ^{32}P] ATP and isotope-unlabelled ATP in kinase buffer (20 mM HEPES (pH 7.4), 1 mM dithiothreitol, 10 mM $MgCl_2$, and 10 mM $MnCl_2$). The incorporated radioactivity was measured by autoradiography. For the non-radioactive kinase assay the phosphorylated substrate was detected by Western blotting. Recombinant β-catenin was used as a positive control substrate for Fyn.

Identification of phosphorylation sites on Fyn-phosphorylated Menin

An in vitro kinase assay was performed as discussed above, replacing [γ^{32}P]ATP with unlabelled ATP. The ABSciex TripleTOF 5600 system (SCIEX) coupled with Eksigent 1D+ Nano LC system (SCIEX) was used to identify Menin's phosphorylated sites. Nano LC of enzymatic peptides was performed with the Eksigent 1D+ Nano LC equipped with the cHiPLC nanoflex system (SCIEX). Peptides were loaded onto the column and then eluted with a linear gradient of 5–40% binary solvent B1 for 30 min at a flow rate of 0.3 mL/min. Mass spectrometry analysis of peptides was performed using the ABSciex TripleTOF 5600 system. Analysis was performed using the NanoSpray III source (SCIEX). The mass spectrometry was calibrated by the acquisition of [Glu1] fibrinopeptide (25 pmol/ml). The raw data were processed and searched with ProteinPilot™ software (version 4.0) using the Paragon algorithm. Proteins were identified by searching the UniProtKB human database and filtered at an R95% confidence cut-off. Peptides for phosphorylated Men1 were identified at a 1% false discovery rate.

Small ubiquitin-like modifier (SUMOylation) assay

We performed the *in vitro* SUMOylation assay with endogenously-expressed or overexpressed proteins. Briefly, HEK 293T cells were transfected with pcDNA3.1-Xpress-*MEN1* (WT or Y603F, Y603D, K493R, K609R mutants) and pcDNA3-HA-*SUMO-1* using iMFectin. 24 h after transfection, cells were lyzed in NP-40 buffer. SUMOylated-Menin proteins were visualized by immunoprecipitation with an Xpress tag or anti-Menin antibody and immunoblotted for HA or SUMO-1 antibodies. We also analyzed SUMOylation of menin by using the EpiQuik™ In Vivo Universal Protein Sumoylation Assay Kit (EPIGENTEK). Briefly, nuclear lysates from transfected HEK 293T cells and mESCs were prepared using NE-PER cytoplasmic and nuclear protein extraction kit (ThermoFisher Scientific). Nuclear lysates (10 µg) were used for the assay. SUMOylation intensity was calculated against a standard curve prepared from recombinant SUMO proteins according to the manufacturer's protocol.

Establishing stable transfectants of mESCs by electroporation

E14TG2a cells (2 x10^8) were co-electroporated with pcDNA3.1-Xpress-*MEN1* (mock, WT or Y603F, Y603D, K609R mutants) and pcDNA3.1-HA-*SUMO-1*. A total of 20 µg of DNA was used at 230 V and 500 mF by the Gene Pulser X (Bio-Rad). Cells were plated onto 60-mm dishes and selected with 1 mg/mL G418 two

days after electroporation. Stable cells were confirmed by immunoblotting with Xpress and HA antibodies. Cells were maintained 12 passages before telomere analysis.

RNA-immunoprecipitation (RNA-IP) and RNP-immunoprecipitation (RNP-IP)

RNA-IP was performed according to Tang et al., 2018[44] with minor modifications. Briefly, cDNA was used as a template to amplify hTERC or mTERC. All 5' primers contained the T7 promoter sequence 5'-CCAAGCTTCTAATACGACTCACTATAGGGAGA-3'. PCR-amplified DNA was used as a template to transcribe biotinylated RNA using T7 RNA polymerase and biotin-UTP. One µg of purified biotinylated transcripts was incubated with 200 µg of nuclear extracts for 60 min at 4°C. Complexes were isolated with streptavidin-conjugated agarose beads (MilliporeSigma), and the pull-down material was analyzed by Western blotting.

For RNP IP assays, cells were exposed to UVC (400 mJ/cm^2), and lysates were prepared in IP buffer (10 mM Hepes, pH 7.4, 50 mM β-glycerophosphate, 1% Triton X-100, 10% glycerol, 2 mM EDTA, 2 mM EGTA, 10 mM NaF, 1 mM DTT, protease inhibitor cocktail, NEM, RNase inhibitor) and immunoprecipitated with anti-Menin or anti-Xpress overnight. The complexes were washed twice with stringent buffer (100 mM Tris-HCl, pH 7.4, 500 mM LiCl, 0.1% Triton X-100, and 1 mM DTT, protease inhibitor cocktail, N-ethylmaleimide, RNase inhibitor) and twice with IP buffer. The RNA in RNP IP was assessed by qRT-PCR analysis and normalized to the *U6* gene[44].

Identification of unknown proteins recruited by Menin on TERC

A proteome-based approach was used for determining the protein targets interacting with SUMOylated-menin and TERC binding. First, HEK 293T cells were transfected with *MEN1* mutants (Y603F, Y603D) with HA-tagged *SUMO-1* for 24 h, and nuclear lysates were subjected to RNA-IP. Differential protein expression across the samples was screened by conducting MS/MSALL with SWATHTM acquisition. The raw data were collected through Information Dependent Acquisition (IDA) and SWATHTM acquisition using ABSciex TripleTOF^{TM} 5600 with Eksigent 1D+ nano LC (nanoLC-MS/MS instrument). Protein identification, MS peak extraction, and statistical analysis were performed with ProeinPilot^{TM} (version 4.5), PeakView^{TM} (version 2.2) and MarkerView^{TM} (version 1.2), respectively. Bioinformatics analyses were conducted with the BioVenn program [45] [45] and displayed in a Venn-diagram of differential expressed proteins. Protein classification was performed using the String software (https://string-db.org) and GraphPad prism 8.0 was used to make the pie diagram.

Bone marrow isolation and hematoxylin and eosin staining

Bone marrow specimens were fixed in acetic acid–zinc–formalin fixative, decalcified in 10% formic acid–5% formaldehyde, and processed for paraffin embedding. The 1.5 µM paraffin-embedded sections were stained with H&E and the morphology visualized by Nikon light microscopy.

Generation of Fyn knockout DC-iPS cells using CRISPR-Cas9

CRISPR-Cas9-mediated genome editing was performed transfecting DC fibroblasts with Fyn and control Double Nickase human Plasmids (Santa Cruz Biotechnology). according to the manufacturer's protocol. Immunoblots confirmed gene knockout efficiency.

pY603-menin antibody validation

The specificity of custom purified pTyr603-menin (pY603-menin) rabbit polyclonal antibody (Abclonal) was confirmed by using phospho-blocking peptides. Further validation was performed by using *in vitro* kinase assays.

Immunofluorescence-FISH (IF-FISH) assay

Metaphase spreads were prepared as described above. Slides were fixed in 4% paraformaldehyde at room temperature for 10 min, followed by permeabilization with 0.05% Triton-x100 for 10 min. Slides were blocked in 5% serum for 1 h, incubated overnight with a primary antibody, and incubated with a fluorochrome-tagged secondary antibody for 1 h. The same slides were subjected to FISH assay using telomeric PNA probes as described above.

Statistical analysis

Data were analyzed either by student's t-test or by one-way analysis of variance (ANOVA) followed by Tukey multiple comparisons test using the GraphPad Prism software. A probability of $p < 0.05$ was considered statistically significant. Each experiment was performed at least 3 times unless otherwise indicated. *$p \leq 0.05$, **$p \leq 0.01$, and ***$p \leq 0.001$.

Declarations

Acknowledgments

The authors thanks Tara Adams and Teri Bishop Johnson for their help to handle animal colonies, Josh Monte and Todd Schuster for their help in Flow-FISH analysis. This work was supported by The Hormel Foundation.

Author Contributions

S.P. developed, execute and supervised the idea and project, performed most of the experiments and data analysis, and wrote the manuscript. P.M contributes in writing and editing of the manuscript. L.T.M.L purified recombinant proteins and helped with cloning. J.H.R performed Tandem Mass spectrometry analysis. W.C and A.M.B reviewed and edited the manuscript. R.C-G reviewed and edited the manuscript and helped S.P to execute the project. Z.D. directed the project and reviewed the manuscript.

Conflict of Interest

Authors declare no conflict of interest.

Data and Materials Availability

Further information and requests for resources and reagents should be directed to and will be fulfilled by the corresponding author, Souren Paul and co-corresponding authors Rafael Contreras-Galindo and Zigang Dong. All unique materials generated in this study are available from the corresponding authors with reasonable request.

References

1. Shay, J. W. & Wright, W. E. Hallmarks of telomeres in ageing research. Journal of Pathology vol. 211 114–123 (2007).
2. Shay, J. W. Telomeres and aging. Current Opinion in Cell Biology vol. 52 1–7 (2018).
3. Hiyama, E. & Hiyama, K. Telomere and telomerase in stem cells. Br. J. Cancer **96**, 1020–1024 (2007).
4. Kirwan, M. & Dokal, I. Dyskeratosis congenita, stem cells and telomeres. Biochimica et Biophysica Acta - Molecular Basis of Disease vol. 1792 (2009).
5. Kam, M. L. W., Nguyen, T. T. T. & Ngeow, J. Y. Y. Telomere biology disorders. npj Genom. Med. 6, 36 (2021). https://doi.org/10.1038/s41525-021-00198-5.
6. Gaspar, T. B. *et al.* Telomere maintenance mechanisms in cancer. Genes (Basel). **9**, (2018).
7. Lee, S. S., Bohrson, C., Pike, A. M., Wheelan, S. J. & Greider, C. W. ATM Kinase Is Required for Telomere Elongation in Mouse and Human Cells. Cell Rep. **13**, 1623–1632 (2015).
8. Tong, A. S. *et al.* ATM and ATR Signaling Regulate the Recruitment of Human Telomerase to Telomeres. Cell Rep. **13**, 1633–1646 (2015).
9. Kim, J. E. *et al.* Fyn is a redox sensor involved in solar ultraviolet light-induced signal transduction in skin carcinogenesis. Oncogene **35**, (2016).
10. Saito, Y. D., Jensen, A. R., Salgia, R. & Posadas, E. M. Fyn: A novel molecular target in cancer. Cancer vol. 116 1629–1637 (2010).
11. Meyn, M. A., Schreiner, S. J., Dumitrescu, T. P., Nau, G. J. & Smithgall, T. E. Src family kinase activity is required for murine embryonic stem cell growth and differentiation. Mol. Pharmacol. **68**, 1320–1330 (2005).
12. Zhang, X., Simerly, C., Hartnett, C., Schatten, G. & Smithgall, T. E. Src-family tyrosine kinase activities are essential for differentiation of human embryonic stem cells. Stem Cell Res. 379–389 (2014) doi:10.1016/j.scr.2014.09.007.
13. Katona, B. W., Glynn, R. A., Hojnacki, T. A. & Hua, X. Menin: Expanding and dichotomous roles in cancer. *Oncoscience* **6**, (2019).
14. Suphapeetiporn, K., Greally, J. M., Walpita, D., Ashley, T. & Bale, A. E. MEN1 tumor-suppressor protein localizes to telomeres during meiosis. Genes Chromosom. Cancer **35**, (2002).
15. Blanpain, C. & Fuchs, E. Epidermal Stem Cells of the Skin. Annu Rev Cell Dev Biol. **22**:339–73 (2006).

16. Andersson-Rolf, A., Zilbauer, M., Koo, B. K. & Clevers, H. Stem cells in repair of gastrointestinal epithelia. *Physiology* vol. 32 278–289 (2017).
17. Skvortsov, D. A., Zvereva, M. E., Shpanchenko, O. V & Dontsova, O. A. Assays for Detection of Telomerase Activity. Acta Naturae **3**, (2011).
18. Podlevsky, J. D. & Chen, J. J. L. It all comes together at the ends: Telomerase structure, function, and biogenesis. Mutation Research - Fundamental and Molecular Mechanisms of Mutagenesis vol. 730 (2012).
19. Ramlee, M. K., Wang, J., Toh, W. X. & Li, S. Transcription regulation of the human telomerase reverse transcriptase (hTERT) gene. *Genes* vol. 7 (2016).
20. Hashimoto, M. *et al.* Role of menin in the regulation of telomerase activity in normal and cancer cells. Int. J. Oncol. **33**, 333–340 (2008).
21. Geiss-Friedlander, R. & Melchior, F. Concepts in sumoylation: A decade on. Nature Reviews Molecular Cell Biology vol. 8 (2007).
22. Hietakangas, V. *et al. PDSM, a motif for phosphorylation-dependent SUMO modification*. 10.1073pnas.0503698102 (2005).
23. Feng, Z.-J., Gurung, B., Jin, G.-H., Yang, X.-L. & Hua, X.-X. *SUMO modification of menin*. *Am J Cancer Res* vol. 3 www.ajcr.us/ISSN:2156-6976/ajcr0000160 (2013).
24. Zhao, Q. *et al.* GPS-SUMO: A tool for the prediction of sumoylation sites and SUMO-interaction motifs. Nucleic Acids Res. **42**, (2014).
25. Roake, C. M. & Artandi, S. E. Regulation of human telomerase in homeostasis and disease. Nat. Rev. Mol. Cell Biol. **21**, 384–397 (2020).
26. Stoopler, E. T. & Shanti, R. M. Dyskeratosis Congenita. *Mayo Clin. Proc.* **94**, 1668–1669 (2019).
27. Frescas, D. & de Lange, T. A TIN2 dyskeratosis congenita mutation causes telomerase-independent telomere shortening in mice. Genes and Development vol. 28 153–166 (2014).
28. Piedra, J. *et al.* p120 Catenin-Associated Fer and Fyn Tyrosine Kinases Regulate β-Catenin Tyr-142 Phosphorylation and β-Catenin-α-Catenin Interaction. Mol. Cell. Biol. **23**, 2287–2297 (2003).
29. Nygaard, H. B. Targeting Fyn Kinase in Alzheimer's Disease. Biol. Psychiatry **83**, 369–376 (2018).
30. Collins, K. The biogenesis and regulation of telomerase holoenzymes. Nature Reviews Molecular Cell Biology vol. 7 (2006).
31. Nagpal, N. *et al.* Small-Molecule PAPD5 Inhibitors Restore Telomerase Activity in Patient Stem Cells. Cell Stem Cell **26**, 896–909.e8 (2020).
32. Mitchell, J. R., Wood, E. & Collins, K. A telomerase component is defective in the human disease dyskeratosis congenita. Nature **402**, (1999).
33. Ayas, M. & Ahmed, S. O. Dyskeratosis Congenita. in *Congenital and Acquired Bone Marrow Failure* 225–233 (Elsevier Inc., 2017). doi:10.1016/B978-0-12-804152-9.00018-X.
34. Espejel, S. & Blasco, M. A. Identification of telomere-dependent 'senescence-like' arrest in mouse embryonic fibroblasts. Exp. Cell Res. **276**, (2002).

35. Stein, P. L., Lee, H. M., Rich, S. & Soriano, P. pp59fyn mutant mice display differential signaling in thymocytes and peripheral T cells. Cell **70**, (1992).
36. Bryja, V., Bonilla, S. & Arenas, E. Derivation of mouse embryonic stem cells. Nat. Protoc. **1**, 2082–2087 (2006).
37. Hanke, J. H. *et al. Discovery of a Novel, Potent, and Src Family-selective Tyrosine Kinase Inhibitor STUDY OF Lck-AND FynT-DEPENDENT T CELL ACTIVATION**. http://www.jbc.org/ (1996).
38. Durkin, M. E., Qian, X., Popescu, N. C., & Lowy, D. R.. Isolation of Mouse Embryo Fibroblasts. Bio-protocol, **3**(18) (2013).
39. Canela, A. S., Vera, E., Klatt, P. & Blasco, M. A. *High-throughput telomere length quantification by FISH and its application to human population studies*. 10.1073pnas.0609367104 (2007).
40. Mourkioti, F. *et al.* Role of telomere dysfunction in cardiac failure in Duchenne muscular dystrophy. Nat. Cell Biol. **15**, 895–904 (2013).
41. Schmid, I. & Jamieson, B. D. Assessment of Telomere Length, Phenotype, and DNA Content. *Curr. Protoc. Cytom.* **29**, 7.26.1–7.26.13 (2004).
42. Wang, F. *et al.* Robust measurement of telomere length in single cells. *Proc. Natl. Acad. Sci. U. S. A.* **110**, (2013).
43. Rueden, C. T. *et al.* ImageJ2: ImageJ for the next generation of scientific image data. BMC Bioinformatics **18**, (2017).
44. Tang, H. *et al.* HuR regulates telomerase activity through TERC methylation. Nat. Commun. **9**, (2018).
45. Hulsen, T., de Vlieg, J. & Alkema, W. BioVenn - A web application for the comparison and visualization of biological lists using area-proportional Venn diagrams. BMC Genomics **9**, (2008).

Figures

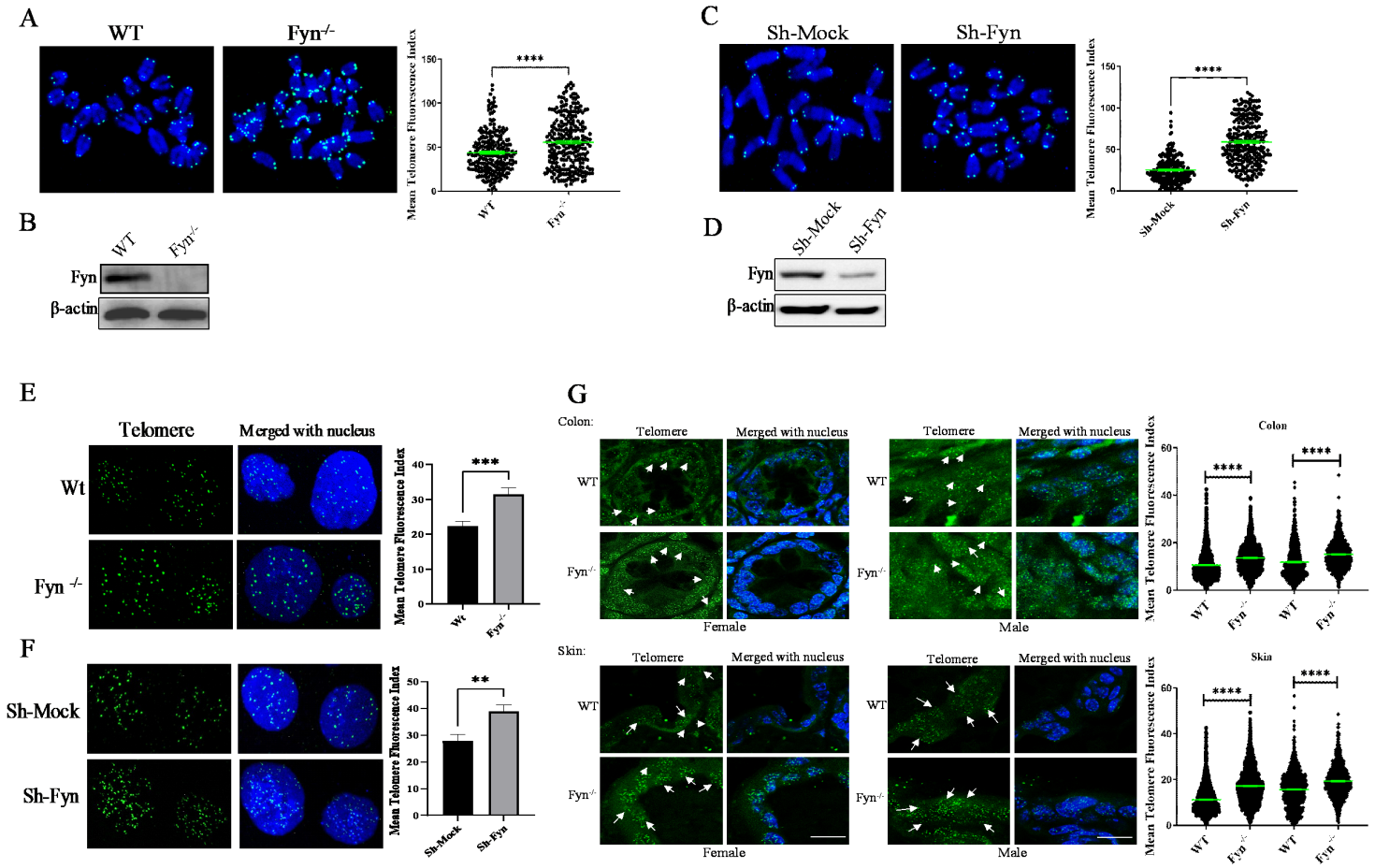

Figure 1

Fyn inhibition promotes telomere maintenance in mESCs

(A, C) Representative images of Q-FISH telomere analysis of metaphase chromosomes of mESCs (P12) isolated from (A) WT and Fyn$^{-/-}$ mice and (C) stable sh-mock and sh-Fyn E14 (P18) cells (n = 20 metaphase spreads). Differences in the Mean Telomere Fluorescent Index (n= 400 telomeres) are shown at the right of each figure.

(B, D) Western blotting of Fyn in (B) WT and Fyn KO mESCs and (D) sh-mock and sh-Fyn cells. B-actin served as a loading control.

(E, F) Representative images of interphase nuclei Q-FISH analysis (left panel) and quantification using the Telometer program (right panel) in wild type vs Fyn-/- mESCs (P12) (E) and in sh-mock vs sh-Fyn E14 cells (P18) (F), showing higher telomere fluorescence in Fyn deficient conditions. (n=20 interphase nuclei).

(G) Representative images of female and male colon (upper) and skin tissues (lower) from 97-week-old WT and Fyn$^{-/-}$ mice used in Q-FISH analysis (scale 20 μM). Telomere fluorescence signals (Q-FISH) are quantitated in both colon and skin tissues from Fyn KO mice compared to WT irrespective of gender (n = 100 nuclei) using the Telometer program.

Data are presented as means ± SEM from a two-tailed t-test. A probability of $p < 0.05$ was considered statistically significant.

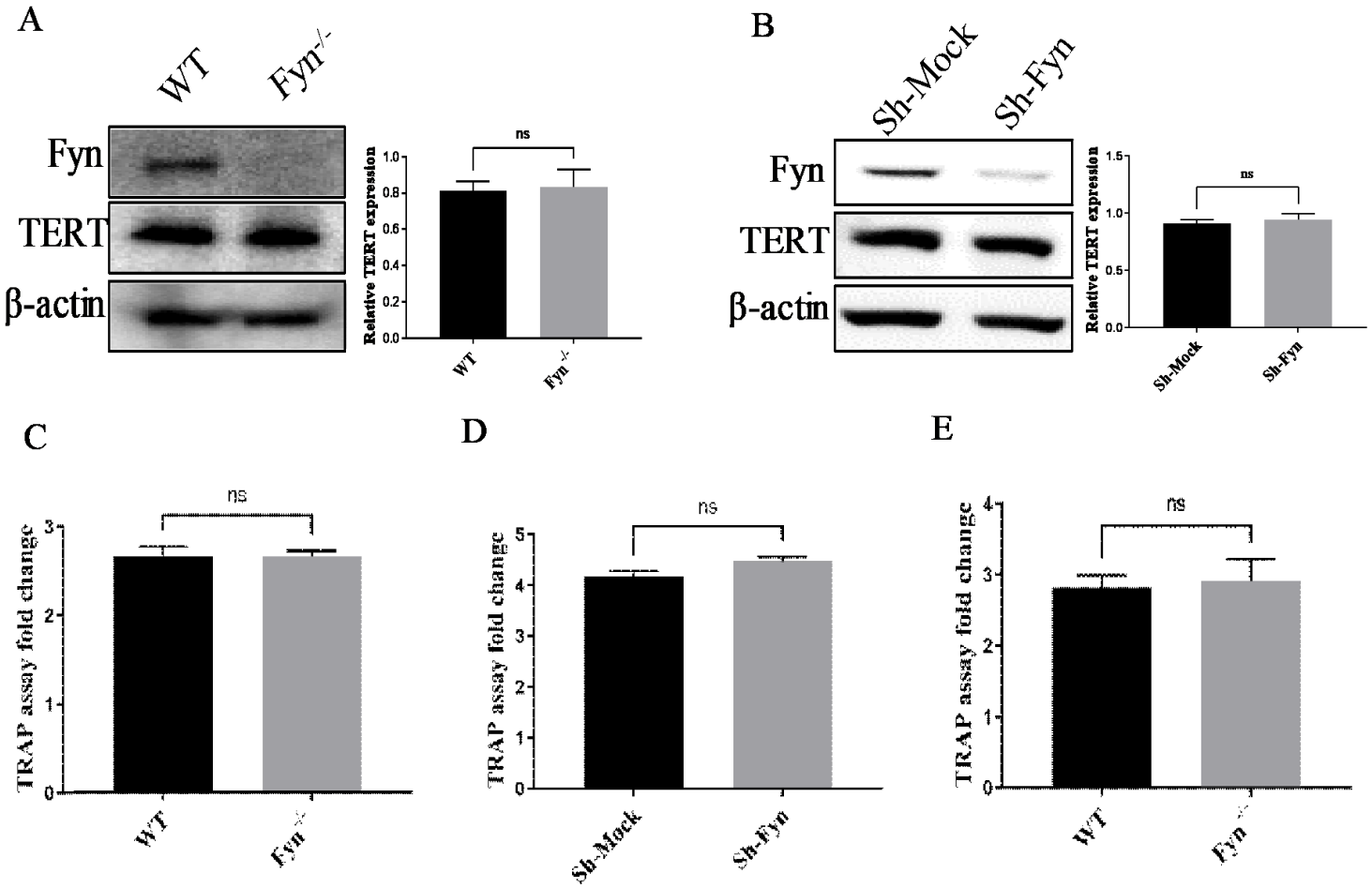

Figure 2

Fyn does not inhibit telomerase activity *in vitro*

(A, B) Western blotting of Fyn and TERT in (A) WT and Fyn KO mESCs and (B) sh-mock and sh-Fyn cells. Actin beta served as a loading control. Densitometry analysis by ImageJ shows no significant difference in TERT expression.

(C, D, E) Telomerase enzyme activity (TRAP assay fold change) was not significantly different between WT and Fyn-/- mESCs (C) or between sh-mock and sh-Fyn E14 cells (D) or in colon of 43-weeks-old WT

vs. Fyn-/- mice (E).

Data are presented as means ± SEM from a two-tailed t-test. A probability of $p < 0.05$ was considered statistically significant.

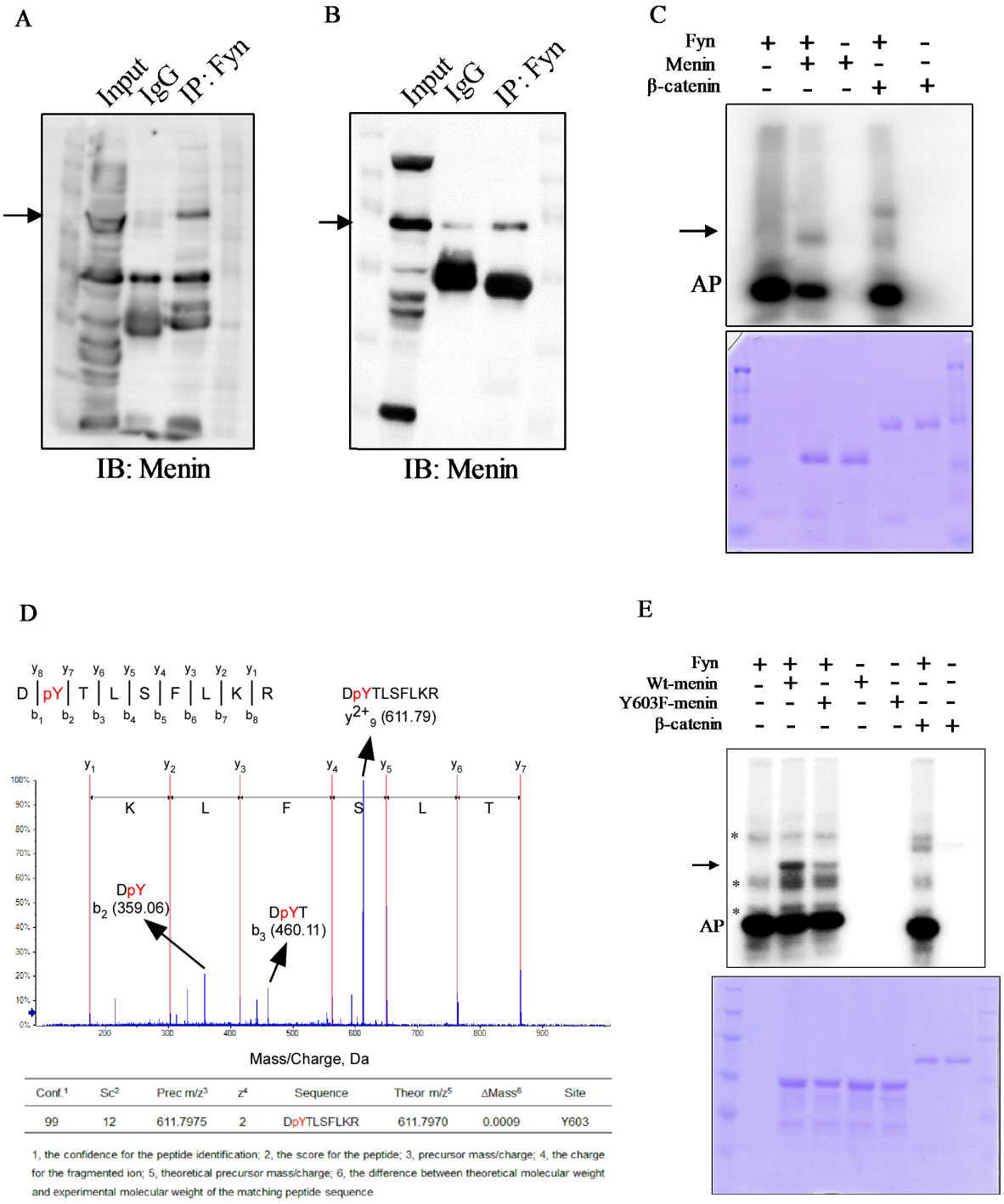

Figure 3

Fyn phosphorylates menin at tyrosine 603

(A and B) Immunoprecipitation using an anti-Fyn antibody followed by Western blotting using anti-menin antibody showing interaction of endogenous Fyn and menin in E14TG2a ES cells (A) and primary mESCs (B).

(C) Active Fyn and full-length menin were subjected to an *in vitro* kinase assay with [γ-^{32}P]ATP. Phosphorylated menin was visualized by autoradiography (indicated by an arrow). Full-length β-catenin was used as a positive control. Menin and β-catenin were stained with Coomassie blue as loading controls (AP; autophosphorylation).

(D) Tandem mass spectrometry spectra of the menin site phosphorylated by Fyn. The precursor mass (m/z) of 611.7975 was matched to the triply charged peptide, DpYTLSFLKR, indicating that Y603 is phosphorylated. The b2 ion at 359.06 and b3 ion at 460.11 indicate that Y603 is phosphorylated.

(E) *In vitro* kinase assay of purified full-length His-menin and His-Y603F-menin by [γ-32P]ATP and active Fyn. Full-length β-catenin is a positive control. The phosphorylated WT and mutant menin were visualized by autoradiography (indicated by arrow, upper). Menin was stained with Coomassie blue as a control (AP; autophosphorylation; * indicates nonspecific bands).

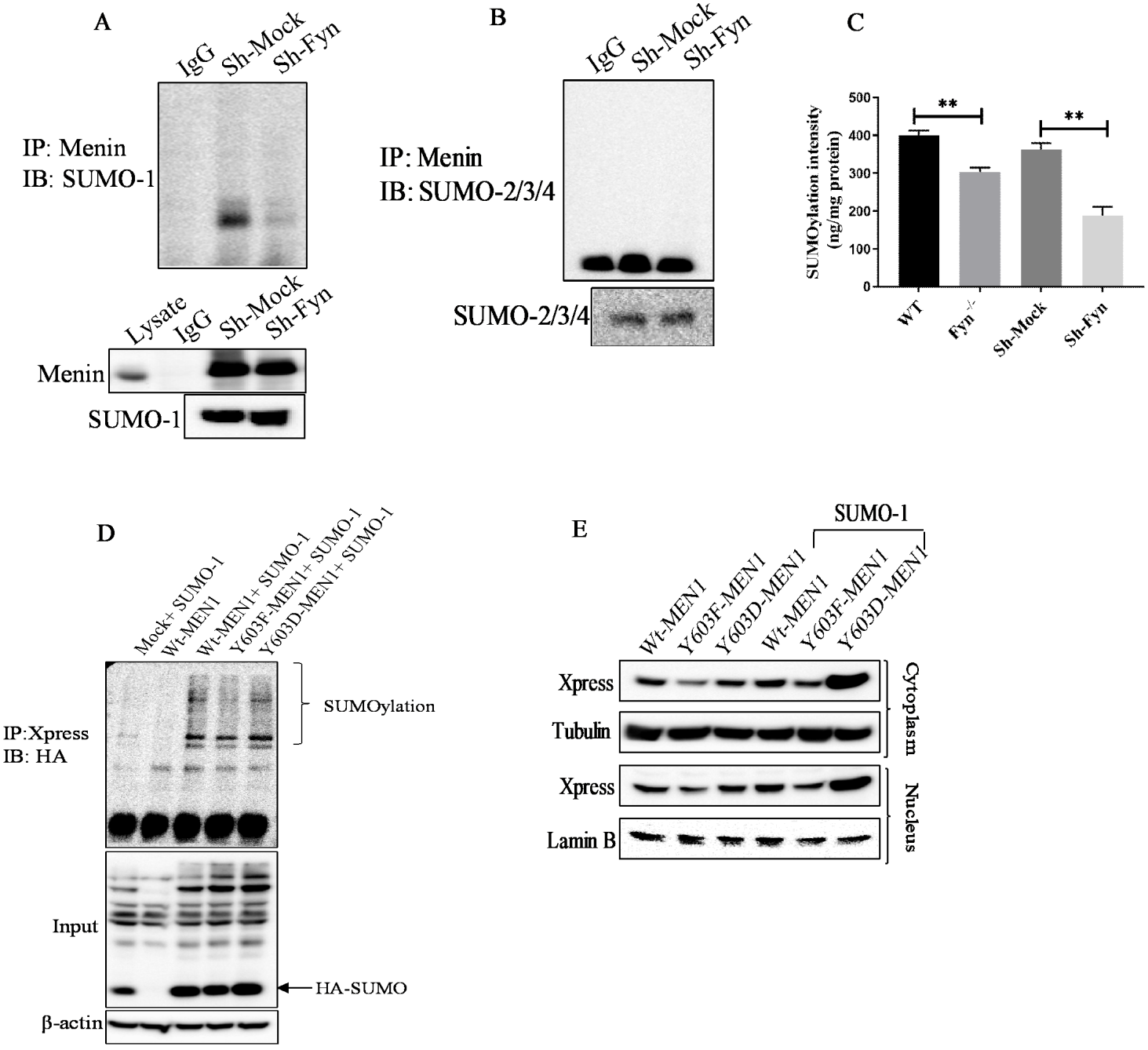

Figure 4

Phosphorylation of menin at Y603 promotes its SUMOylation and stability

(A) Menin and SUMO-1 interaction shown by immunoprecipitation of endogenous menin and Western blotting of SUMO-1 in sh-mock and sh-Fyn E14 cells (upper). Endogenous expression of menin and SUMO-1 in immunoprecipitated samples (lower).

(B) Immunoprecipitation of endogenous Menin and immunoblot against SUMO-2/3/4 in sh-mock and sh-Fyn transfected E14 cells, showing the lack of interaction between menin and SUMO-2/3/4.

(C) SUMOylation is decreased in Fyn-deficient cells as shown by ELISA assays in nuclear lysates of WT and Fyn-/- stem cells or sh-mock and sh-Fyn E14 cells. Data are presented as means ± SEM from a two-tailed t-test. A probability of $p < 0.05$ was considered statistically significant.

(D) A phosphodeficient menin mutant (Y603F) impairs SUMOylation of menin as shown by immunoprecipitation of overexpressed menin (WT, Y603F, Y603D) tagged with Xpress and immunoblotting of overexpressed SUMO-1 tagged with HA in 293T cells.

(E) Western blotting of cytoplasmic and nuclear protein extracts shows that Y603D-MEN1 and SUMO-1promote menin stability. 293T cells were transfected with Xpress-tagged MEN1 (Wt or Y603F, Y603D) with or without HA-tagged SUMO-1 co-transfection.

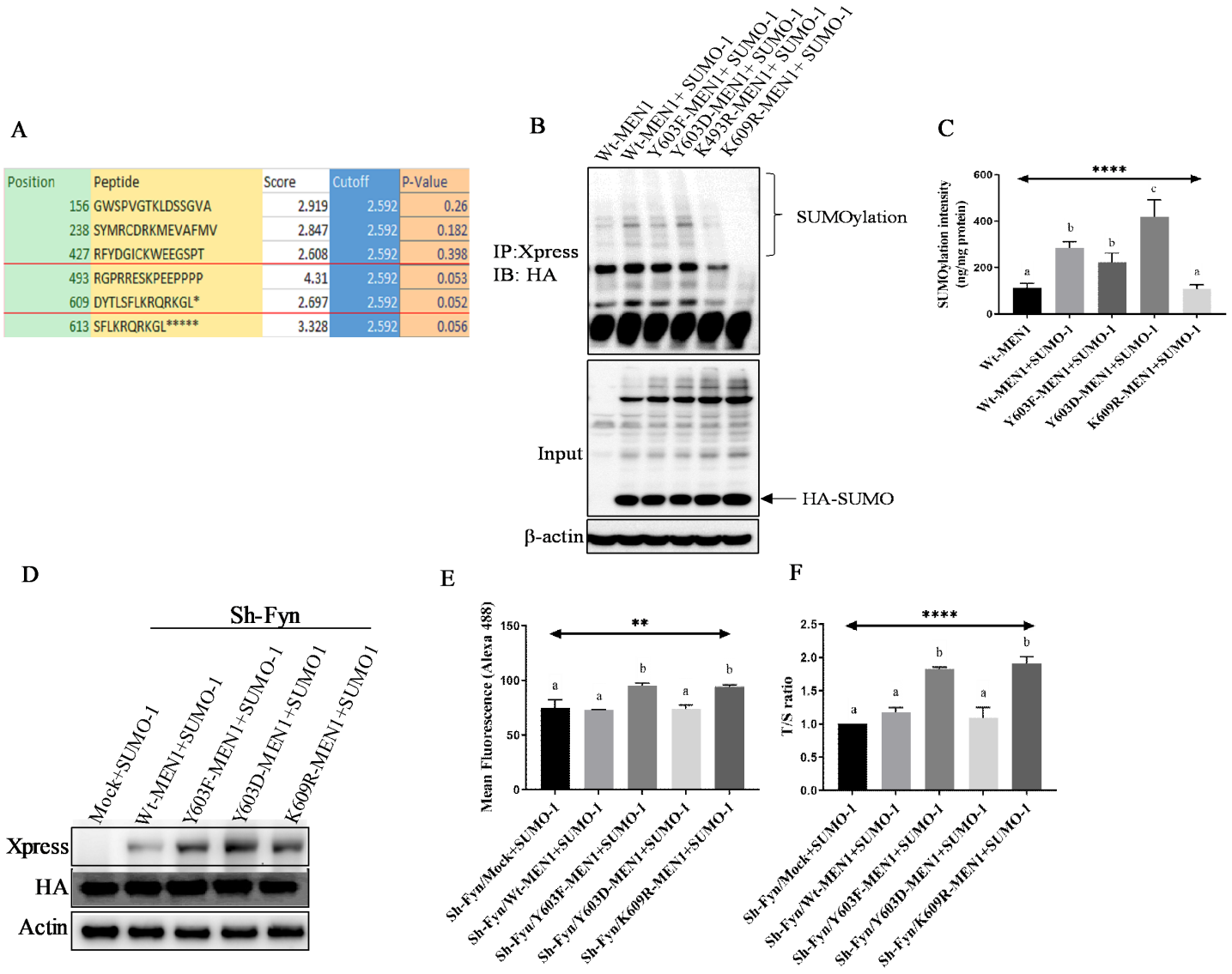

Figure 5

Menin is SUMOylated at lysine 609

(A) Prediction results of menin SUMOylation sites from the GPS-SUMO open-source program.

(B) K609 is a possible SUMO site of menin as shown by co-immunoprecipitation and Western blotting of Xpress-tagged WT and mutant menin proteins with HA-tagged SUMO-1. 293T whole-cell lysates, co-transfected with Xpress-*MEN1* (WT or Y603F, Y603D, K493R, K609R) and HA-*SUMO-1* were immunoprecipitated with mouse Xpress-tag and immunoblotted with HA-HRP.

(C) SUMOylation is decreased in nuclear lysates of K609R-transfected cells as shown by ELISA assay detecting overexpressed WT or mutant MEN1 (Y603F, Y603D, K609R) with SUMO-1 in 293T cells.

(D) Stable electroporated E14 cells harboring mutant MEN1 (Y603F and K609R) exhibit Xpress and HA-HRP bands determined by Western blot.

(E and F) Stable electroporated Fyn-knockdown E14 cells harboring mutant *MEN1* (Y603F and K609R) exhibit elongated telomeres. Flow-FISH analysis (E) and qRT-PCR analysis (F) show higher telomere intensity and higher T/S ratio relative to mouse *36B4* gene in Xpress-Y603F-menin- and Xpress-K609R-menin-transfected cells. Fyn knockdown cells were used in this experiment to lessen Fyn-mediated phosphorylation of endogenous menin and highlight the effect of phospho-site or SUMO-site mutant menin. The cells were passaged 12 times before telomere evaluation.

All data are presented as means ± SEM by a one-way ANOVA followed by Tukey's multiple comparison test. A probability of $p < 0.05$ was considered statistically significant.

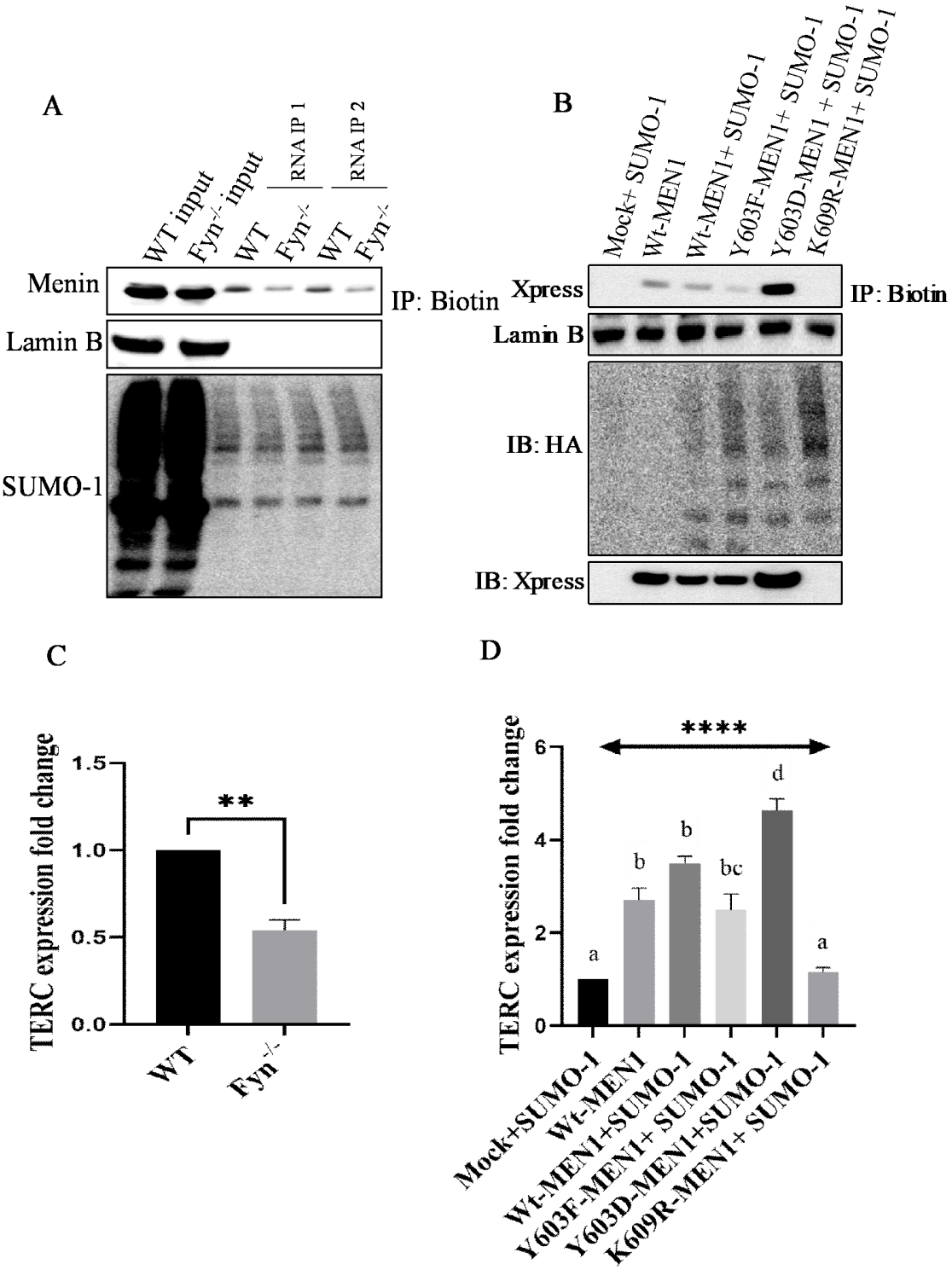

Figure 6

SUMOylated menin is associated with TERC *in vitro*

(A) Western blotting of *in vitro* transcribed RNA pulldown assay using nuclear lysates from WT and Fyn KO mESCs show menin in TERC-associated pulldown complex.

(B) Phosphorylation-dependent SUMOylation is necessary for menin-TERC binding. RNA pulldown assay using *in vitro* transcribed RNA and overexpressed WT or mutant (Y603F, Y603D, K609R) *MEN1* with *SUMO-1* indicates that Y603D menin expression is greatly increased in pulldown complex compared to WT and Y603F menin. K609R menin does not associate with TERC.

(C) RNP pulldown assay with anti-menin antibody followed by qRT-PCR in WT and Fyn$^{-/-}$ mESCs, show increased TERC amplification in WT mESCs vs. Fyn$^{-/-}$ mESCs.

(D) Nuclear lysates from 293T cells transfected with *MEN1* (WT, Y603F, Y603D, K609R) and *SUMO-1* were subjected to RNP-IP with anti-Xpress antibody followed by TERC qRT-PCR. qRT-PCR results show significantly greater TERC amplification in Y603D+SUMO-1 cells vs. WT+SUMO-1 cells. Y603F+SUMO-1 cells show significantly decreased TERC amplification compared to WT-SUMO-1 cells. RNP-IP of K609R+SUMO-1 cells have a further reduction in TERC amplification.

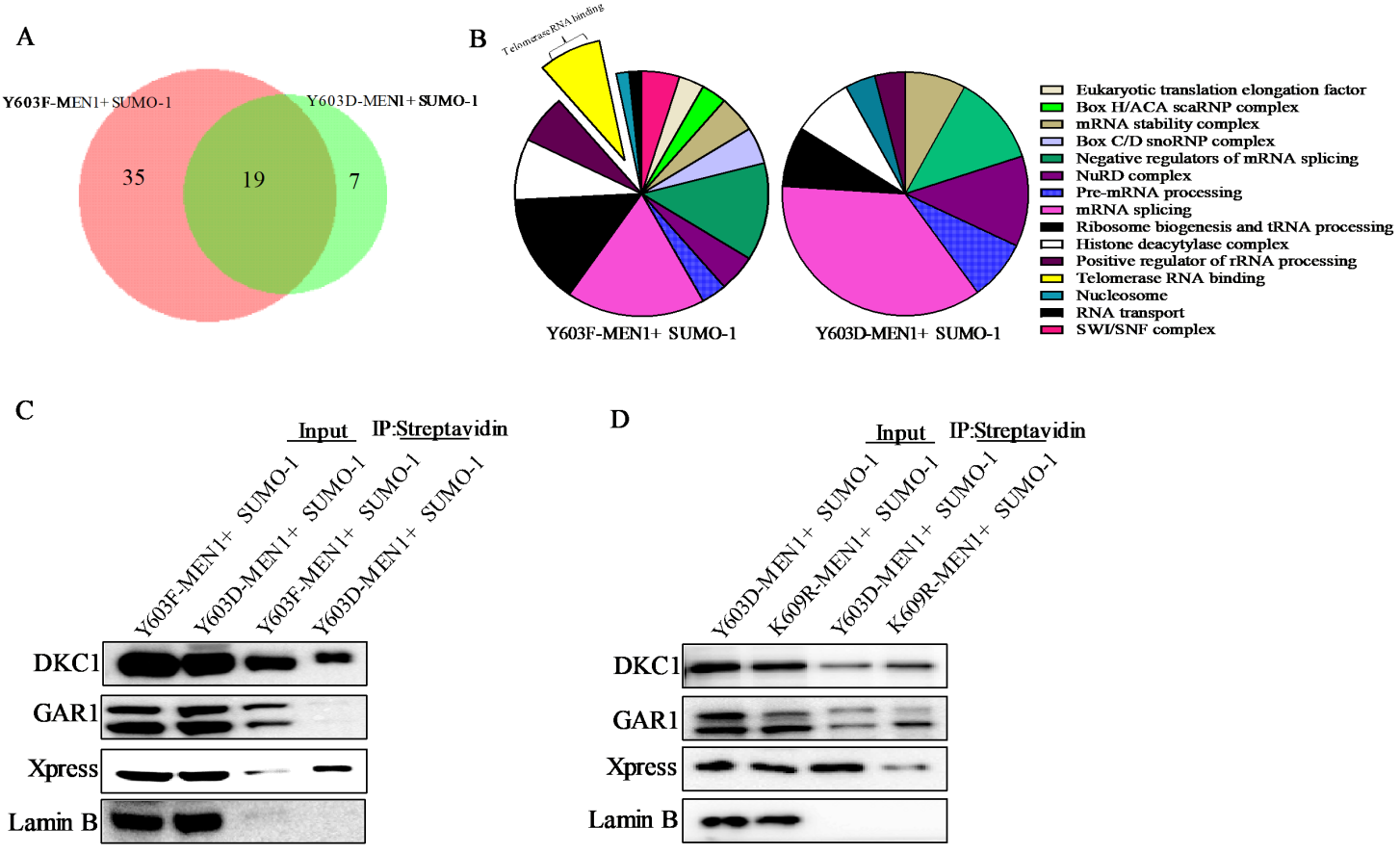

Figure 7

SUMOylated menin prevents recruitment of DKC1 and GAR1 to TERC

(A) A Venn-diagram determined by mass spectrometry analysis displays differential proteins recruited to TERC after Y603F-*MEN1*+*SUMO-1* or Y603D-*MEN1*+SUMO-1 transfection in 293T cells.

(B) A Pie-diagram shows classes of TERC binding proteins in Y603F-MEN1+SUMO-1- and Y603D-MEN1+SUMO-1-transfected 293T cells.

(C) Western blotting of *in vitro* transcribed TERC pulldown assay from nuclear lysates of 293T cells with over-expressed mutant (Y603F, Y603D) menin and SUMO-1 shows decreased DKC1 and GAR1 expression in Y603D+SUMO-1 transfected cells.

(D) Western blotting of *in vitro* transcribed TERC pulldown assay from nuclear lysates of 293T cells with over-expressed mutant (Y603D, K609R) menin and SUMO-1 shows increased DKC1 and GAR1 expression in K609R+SUMO-1 transfected cells. Menin expression is reduced in K609R+SUMO-1 TERC-IP.

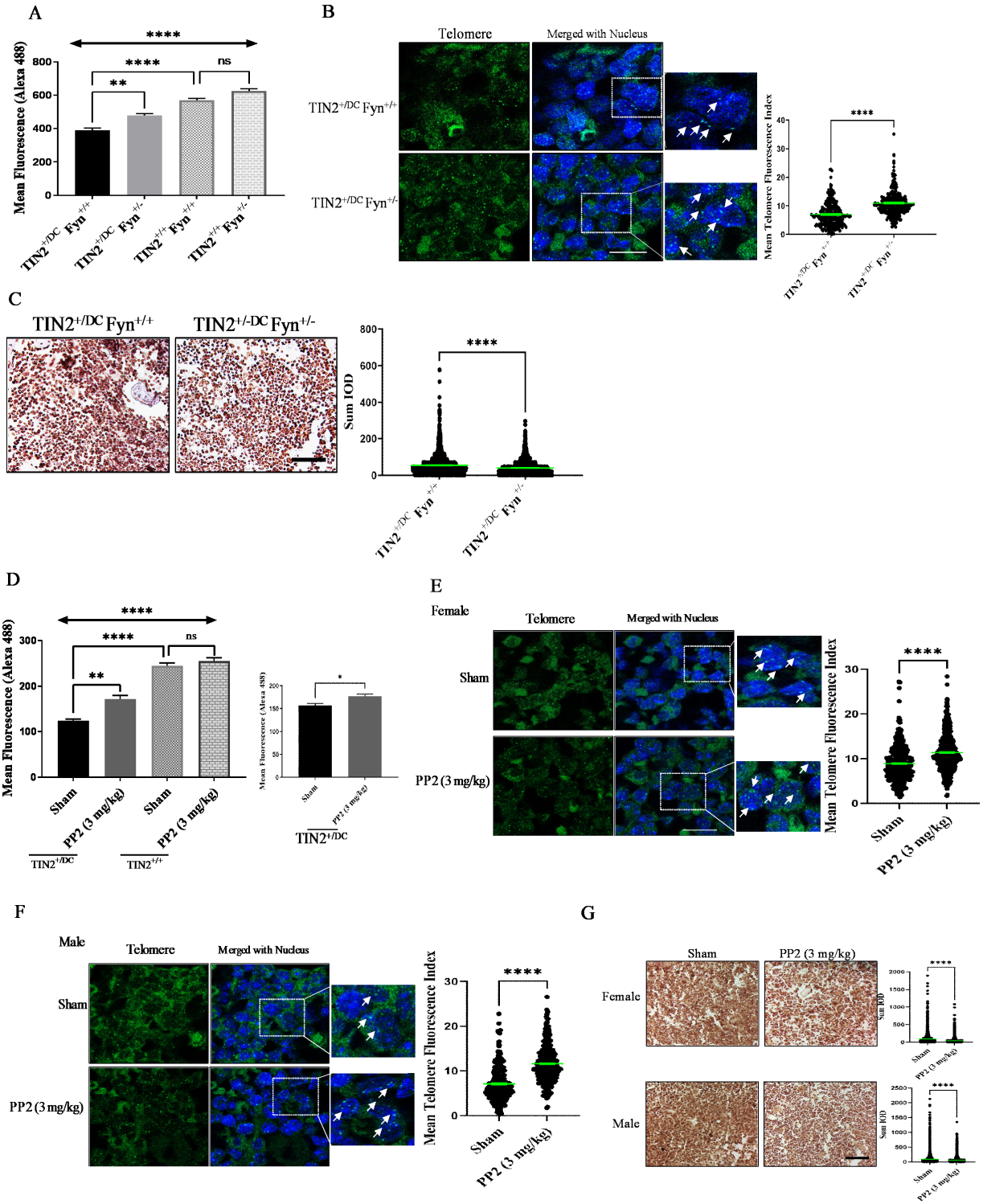

Figure 8

Inhibition of Fyn prevents telomere erosion in TIN2$^{+/DC}$ mice

(A) Flow FISH analysis of total bone marrow cells from TIN2$^{+/DC}$ female mice in the presence or absence of Fyn show TIN2$^{+/DC}$- FYN$^{+/-}$ mice with higher mean telomere fluorescence vs. TIN2$^{+/DC}$-FYN$^{+/+}$ mice.

(B) Representative images of bone marrow tissue Q-FISH analysis (left; right), show $TIN2^{+/DC}$- $FYN^{+/-}$ mouse bone marrow cells with higher FISH signal vs. $TIN2^{+/DC}$- $FYN^{+/+}$ signal (n = 100 nuclei, scale bar 10 μm).

(C) IHC analysis of p-Y603-menin protein expression and quantification by ImageJ in bone marrow tissue biopsy (C) and colon (D) of $TIN2^{+/DC}$- $FYN^{+/-}$ and $TIN2^{+/DC}$-$FYN^{+/+}$ female mice (scale bar 10 μm).

(D) Flow FISH analysis of total bone marrow cells from $TIN2^{+/DC}$ male and female mice after treatment with sham and PP2 (3 mg/kg) shows elongated telomeres in PP2-treated female (left) and male mice (right) vs. sham.

(E and F) Representative images of bone marrow tissue by Q-FISH analysis (left) and quantification (right) in sham- and PP2 (3 mg/kg)- treated female (E) and male (F) mice show PP2-treated bone marrow samples with more telomere signals vs. sham (n = 100 nuclei, scale bar 10 μm).

(G) IHC and ImageJ analyses of pY603-menin protein expression in a bone marrow tissue of $TIN2^{+/DC}$ female and male mice treated with sham and 3 mg/kg PP2 (scale bar 10 μm).

Data (A and D) are shown as means ± SEM by one-way ANOVA and Tukey's multiple comparisons and the rest are shown as means ± SEM by unpaired student t-test. A probability of $p < 0.05$ was considered statistically significant.

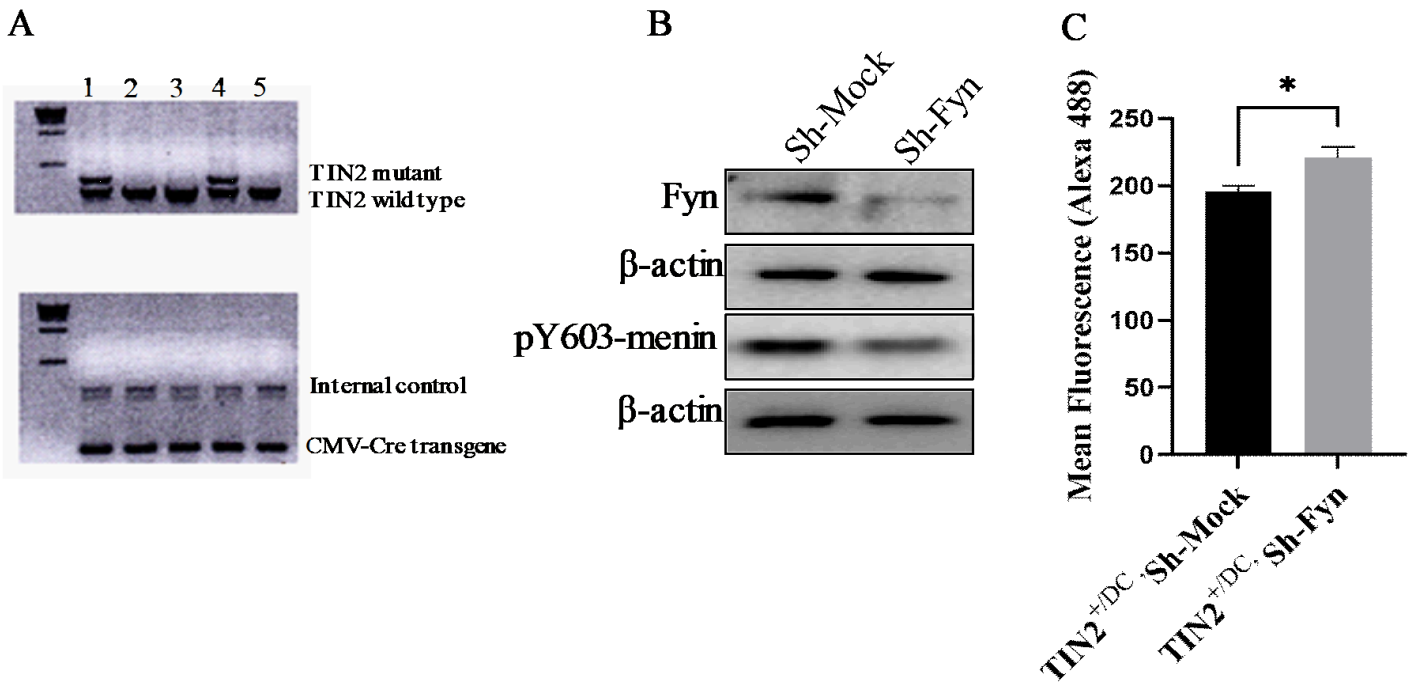

Figure 9

Fyn inhibition attenuates telomere shortening in $TIN2^{+/DC}$ MEFs

(A) Genotyping of isolated MEFs from 5 healthy embryo littermates shows embryos 1 and 4 positive for the TIN2 mutation (upper) and the *Cre* transgene (lower).

(B) Western blotting shows reduced expression of Fyn and pY603-menin in sh-Fyn-transduced $TIN2^{+/DC}$ MEFs vs. mock.

(C) Flow-FISH analysis of stable sh-mock and sh-Fyn $TIN2^{+/DC}$ MEF shows increased mean telomere fluorescence in sh-Fyn $TIN2^{+/DC}$ MEFs vs. sh-mock at passage 6.

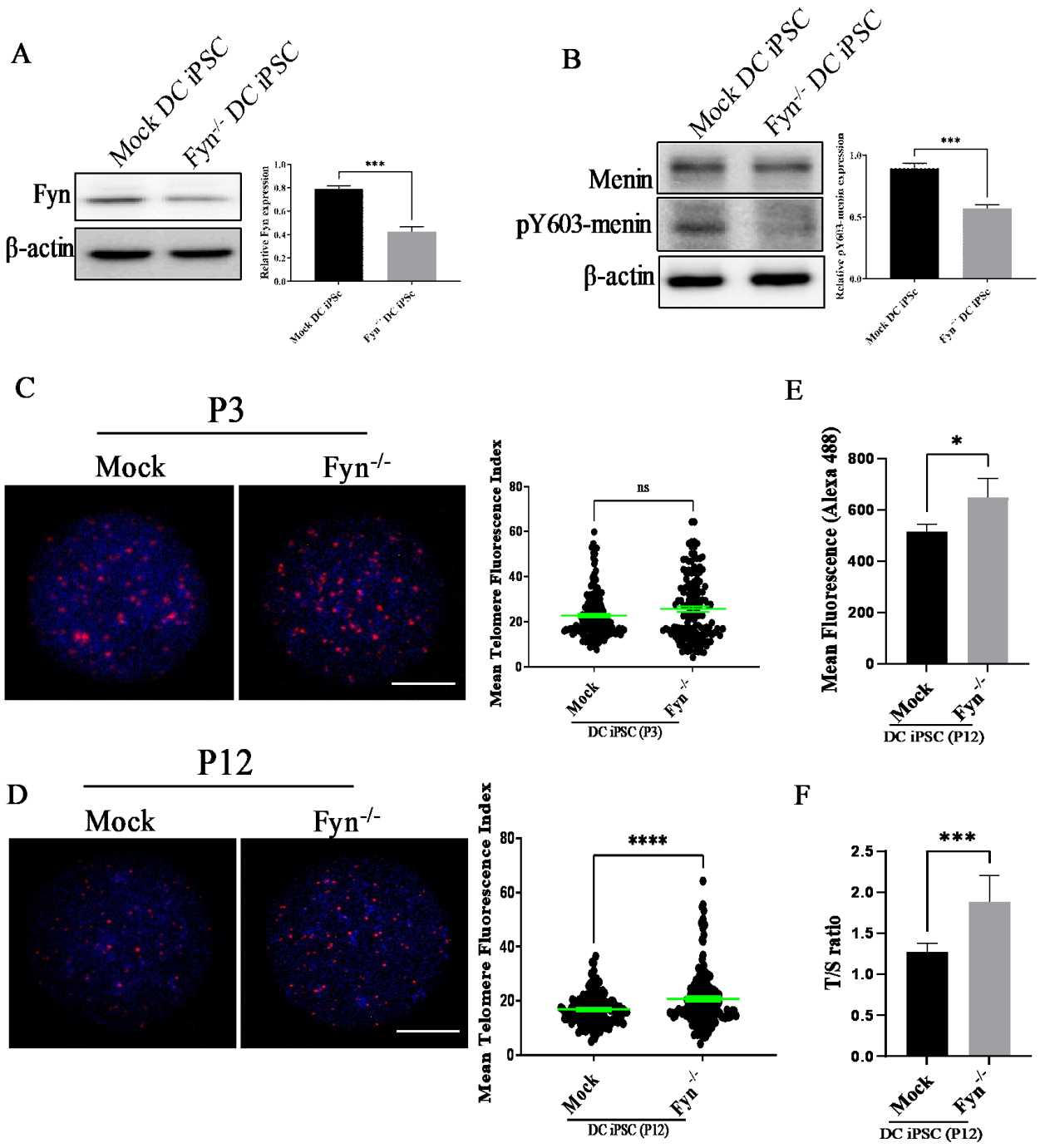

Figure 10

Fyn knockout in Human DC iPSCs attenuates telomere shortening

(A) Western blotting (left) and quantification (right) show CRISPR-Cas9-mediated *Fyn* gene knockdown efficiency in DC iPSCs.

(B) Western blotting (left) and densitometry (right) by ImageJ show reduced expression of pY603-menin in Fyn KO DC iPSC vs. mock DC-iPSC.

(C and D) Representative images of interphase Q-FISH analysis (left) and quantification (right), reveal no significant difference in telomere length at passages 3 of Fyn knockout DC iPSCs vs. mock DC iPSCs (C), but at passages 12, $Fyn^{-/-}$ iPSCs show higher Q-FISH signal vs. mock iPSC (D, n = 50 nuclei).

(E) Flow-FISH analysis shows higher telomeric mean fluorescence in $Fyn^{-/-}$ DC iPSCs vs. mock-DC-iPSCs and (F) qRT-PCR analysis exhibits significantly higher T/S ratio in $Fyn^{-/-}$ DC iPSCs vs. mock-DC-iPSCs (lower). The human *Alu* gene was used for normalization.

Data are presented as means ± SEM from a two-tailed t-test. A probability of $p < 0.05$ was considered statistically significant.

Supplementary Files

This is a list of supplementary files associated with this preprint. Click to download.

- Supplementaryinformationswithfigures.docx